PHILOSOPHICAL TRANSACTIONS OF THE ROYAL SOCIETY A MATHEMATICAL, PHYSICAL & ENGINEERING SCIENCES

Isothermal and Thermo-Osmotic Transport of Sorbable Gases in Microporous Carbon Membranes

R. Ash, R. M. Barrer, J. H. Clint, R. J. Dolphin and C. L. Murray

Phil. Trans. R. Soc. Lond. A 1973 **275**, 255-307
doi: 10.1098/rsta.1973.0101

ISOTHERMAL AND THERMO-OSMOTIC TRANSPORT OF SORBABLE GASES IN MICROPOROUS CARBON MEMBRANES

By R. Ash, R. M. Barrer, F.R.S., J. H. Clint, R. J. Dolphin and C. L. Murray
Physical Chemistry Laboratories, Chemistry Department, Imperial College London SW7 2AY

(*Received 5 February* 1973)

CONTENTS

Vol. 275. A. 1249. 19 [Published 27 September 1973

With the use of helium and a series of gases adsorbed to give dilute films, measurements have been made of thermo-osmotic steady-state pressure ratios established across microporous carbon membranes through which linear temperature gradients were maintained. Two contrasting adsorbents were employed: Carbolac I, a carbon black having an energetically heterogeneous high area surface and Graphon, a graphitized carbon black of one-tenth the surface area of Carbolac but energetically homogeneous. Complementary studies of isothermal transport of the gases through the membranes and determination of equilibrium adsorption isotherms at all temperatures employed for the flow experiments were required in order to analyse the non-isothermal experimental results.

Part I is concerned with the equilibrium properties of the adsorbed films. Henry's law constants, k_s, energies of adsorption, $\Delta E'$ and isosteric heats of adsorption, q'_{st}, for the Gibbs excess adsorption were derived from the experimental isotherms. Taking the thickness of the adsorbed layer as one molecular diameter, the corresponding energies, ΔE, and heats q_{st} for absolute adsorption have been calculated. For the very dilute films the ratios $\Delta E'/\Delta E$ and q'_{st}/q_{st} can differ appreciably from unity. Also in the Henry law range, values of the thermodynamic equilibrium constants and standard energies, $\Delta E^{\ominus}$, and entropies, $\Delta S^{\ominus}$, for absolute adsorption have been evaluated. A linear relation between $\Delta S^{\ominus}$ and $\Delta E^{\ominus}$, was observed. $-\Delta S^{\ominus}$ was considerably larger on Carbolac than on Graphon surfaces. This has been interpreted in terms of greater mobility of the adsorbed molecules on the more homogeneous Graphon surface. Good correlations have been found between K or ΔE and properties, such as polarizability, α, related to the condensability of the sorbates.

Part II is concerned with isothermal transport of the gases through the membranes. For the majority of systems studied the permeability, K and time-lag, L, were independent of pressure. For helium in both membranes the ratio $K/\sqrt{T}$ was independent of temperature and pressure, indicating transport only in the gas phase and the absence of a viscous flow component. For an adsorbed gas the extra flux generated by the mobile adsorbed films per unit area of surface, J_s/A, were considerably greater for the more homogeneous Graphon membrane. Diffusion coefficients associated with the extra fluxes also indicated greater mobility of adsorbed molecules on the more homogeneous surface. Good correlations between $K(M/T)^{\frac{1}{2}}$ and k_s have been demonstrated and, at constant temperature, a linear relation was observed between $KM^{\frac{1}{2}}$ and the product, αT_b, of polarizability and boiling-point T_b. Gas-phase structure factors obtained by the procedure of Barrer & Gabor (1959) were considerably less than unity, indicating a dominant influence in each membrane of tortuosity and bottlenecks. For each membrane a linear relation has been demonstrated between the products KL and k_s from which parameters associated with blind pore character have been obtained.

Part III is concerned with the thermo-osmotic transport of the gases in the membranes. The non-isothermal flow is formulated in terms of the thermodynamics of irreversible processes and relations derived between the straight phenomenological coefficients of this treatment and the permeabilities and diffusion coefficients of part II. Equations are also presented relating the overall heat of transport, Q_0, at temperature T_0 to component heats of transport for the gas-phase flow (Q_g, Q_g^*) and extra flow (Q_s, Q_s^*). In none of the systems studied did $Q_0 = -\frac{1}{2}RT_0$, the ideal value expected for a gas transported by molecular streaming (Knudsen flow). For He, H_2 and Ne in the Carbolac membranes, $Q_0 = -\frac{1}{2}\beta RT_0$ where β, for a particular gas, is a constant < 1. With increasing sorbability of the flowing gas the temperature dependence of Q_0 was progressively modified until, in the presence of substantial extra flow, $-Q_0$ decreased strongly

with increasing T_0. Calculations of Q_s and Q_s^* are presented for the two limiting cases $Q_g = -\frac{1}{2}RT_0$ and $Q_g = 0$. It is shown that Q_s must always be negative and Q_s^* positive. A procedure for calculating isobaric permeabilities, utilizing a combination of thermo-osmotic steady-state and isothermal steady-state measurements, has been developed. For various pairs of gases, the ratios of isobaric permeabilities differed greatly from the corresponding ratios of isothermal permeabilities. Enhanced separations of sorbable mixtures by isobaric flow appear to be possible especially for the Graphon membrane.

I. Adsorbed films at equilibrium

I. 1. *Introduction*

Supported microporous membranes made by compacting high-area carbon powders prove to be very stable both thermally and mechanically (Ash, Barrer & Pope 1963*a*), and can give large 'surface' flows of adsorbable gases which may dominate gas phase transport (Ash, Baker & Barrer 1967). This makes such membranes selective in gas or vapour separations (Ash, Barrer & Pope 1963*b*) and hence of considerable interest. Moreover, the flows can yield much information about the nature of the surfaces, particularly where adsorbed populations of molecules are also measured (Barrer 1967, 1970). For this study carbons of two kinds were used. One of these (Carbolac) consisted of particles with a very high surface area per gram; in the second (Graphon) the particles had much smaller areas per gram and smooth, non-porous surfaces. Although of smaller surface area membranes made of Graphon have been shown to generate fluxes of adsorbed molecules which, per unit area of surface, are considerably larger than those on Carbolac (Ash *et al.* 1967). This behaviour reflects differences in the mobilities of adsorbed molecules which could be reflected in such equilibrium properties as the entropy.

I. 2. *Experimental*

Pure He, Ne, Ar, H_2, N_2, CO and CO_2 were 'grade X' gases supplied by the British Oxygen Co., who also provided Kr and Xe of purity between 99 and 100 %. D_2, 99.5 % pure, was obtained from Cambrian Chemicals Ltd. CH_4, C_2H_6 and C_3H_8 of 99.9 % purity were obtained from the National Physical Laboratory.

The Carbolac and Graphon carbons were obtained from G. L. Cabot Ltd. The adsorption samples were prepared as described elsewhere (Barrer & Gabor 1960) by pressing increments of the required carbon in a split-plug holder held within a cylindrical steel tube. Pellets could thus be obtained with porosity closely approximating that of the microporous membrane of the same carbon (0.47 to 0.48 cm^3 per cm^3 for Carbolac and 0.42 cm^3 per cm^3 for Graphon), used in the study of isothermal (part II) and thermo-osmotic flows (part III). The carbon pellets were given the same outgassing treatments as the membranes, that is they were outgassed for 12 h at room temperature, 50, 100 and 150 °C and for 60 h at 200 °C. After each isotherm measurement the carbons were further outgassed at 200 °C for a minimum of 24 h. With Carbolac pellets the initial outgassing removed 9.4 % by weight, against the makers' evaluation of 16 % total volatile content. Thus some oxygen surface complex remains, and may contribute to the heterogeneity of the sorbent. With Graphon no measurable weight loss was found on degassing at 200 °C.

On the basis of a surface area for N_2 of 0.162 nm^2, the surface area of the pellets of Carbolac was 940 $m^2 g^{-1}$, close to the makers' figure of 950 $m^2 g^{-1}$ for the free powder. The surface area for the Graphon pellets was reported earlier (Ash *et al.* 1967) as 79 $m^2 g^{-1}$. Isotherms were determined volumetrically. Pressures were measured using a cathetometer and mercury manometers with 10 mm precision bore tubing. Gas burettes were jacketed with water circulating from a large

thermostat tank. The volumes of the bulbs in the burettes were measured with mercury and other volumes with helium. The sorption bulbs were thermostatted in baths of silicone oil and pressures were never low enough to require thermal transpiration corrections. For the more strongly sorbed gases the outgassed weight of the Carbolac pellets was 1.097 g but for H_2 and Ne 9.432 g were used. The Graphon pellets weighed 7.164 g.

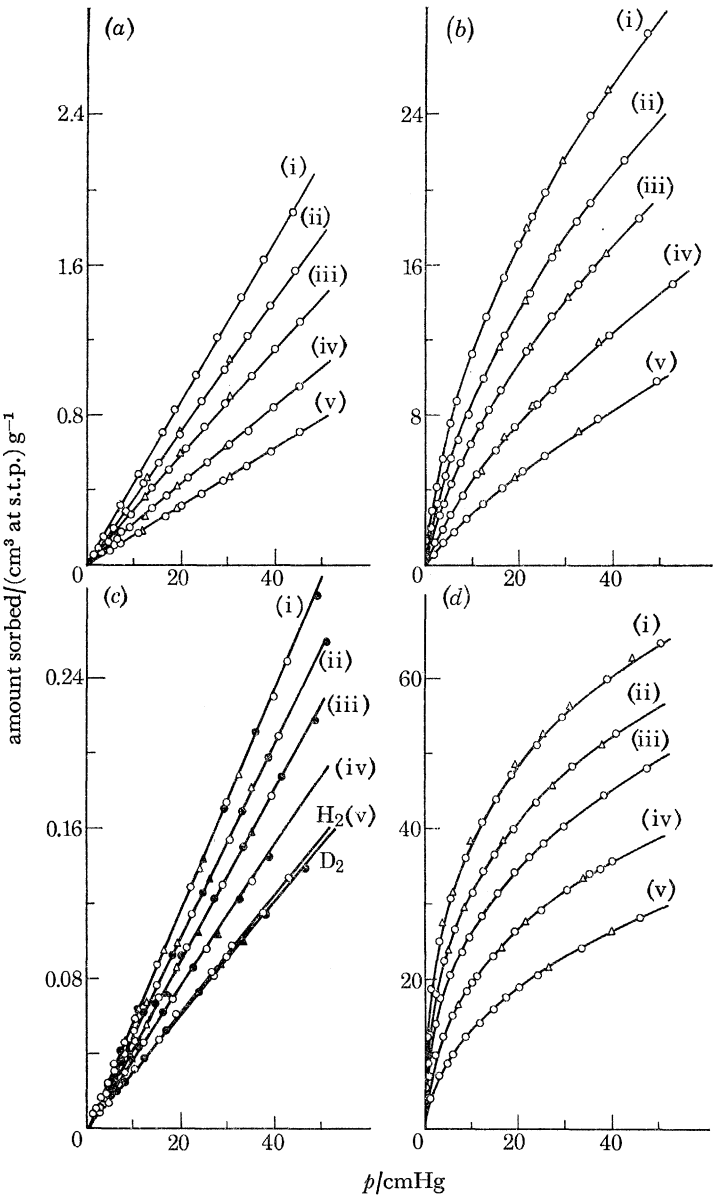

FIGURE I.1. Typical adsorption isotherms on Carbolac at (i) 308.15 K, (ii) 320.65 K, (iii) 333.15 K, (iv) 352.90 K, (v) 378.00 K. (*a*) Ar, (*b*) Xe, (*c*) H_2 (○, △) and D_2 (●, ▲), (*d*) C_3H_8. ○, ●, Adsorption points; △, ▲, desorption points.

I.3. *Results*

I.3.1. *Isotherms*

Typical isotherms are illustrated for Carbolac in figure I.1 and for Graphon in figure I.2. All isotherms were reversible and hence well suited to analysis.

I. 3.2. *The Henry law distribution constants*

The isotherms of H_2, D_2 and Ne on Carbolac and of H_2, Ar, N_2 and CH_4 on Graphon did not deviate measurably from Henry's law, while those of Ar, Kr and CH_4 on Carbolac and of Kr and Xe on Graphon were also near to straight lines. For curved isotherms the limiting slopes were obtained as the amounts sorbed tended to zero. The Henry law constant, k_s, for the Gibbs excess distribution of gas between the surface and the gas phase is conveniently defined as

$$k_s = \frac{C'_s}{C'_g} = \frac{v}{p}\frac{76T}{273.15A_g}. \qquad (I.\,1)$$

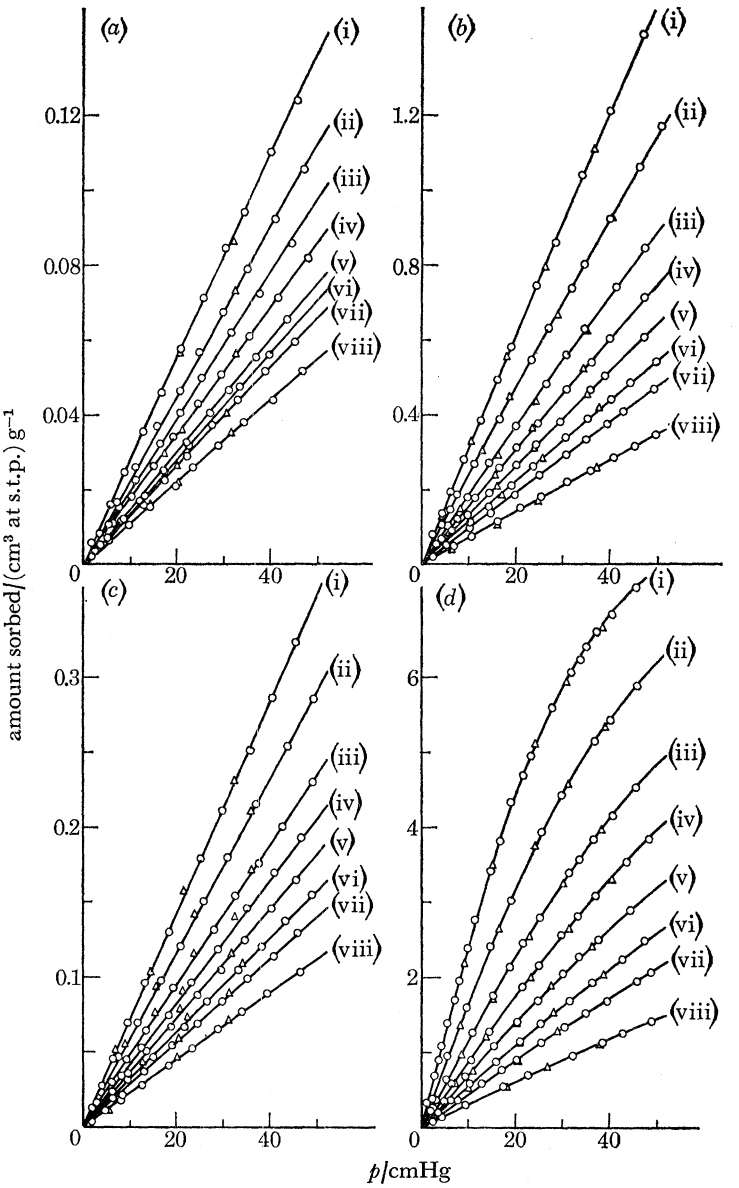

FIGURE I. 2. Typical adsorption isotherms on Graphon at (i) 308.15 K, (ii) 320.65 K, (iii) 333.15 K, (iv) 343.15 K, (v) 353.15 K, (vi) 363.15 K, (vii) 373.15 K, (viii) 393.15 K. (*a*) Ar, (*b*) Xe, (*c*) CH_4, (*d*) C_3H_8. ○, Adsorption points; △, desorption points.

In this expression C'_s denotes the Gibbs excess number of adsorbed molecules per unit area (1 cm^2), C'_g is the number of molecules per unit volume (1 cm^3) of gas phase at the equilibrium temperature T and pressure p in cmHg (1 cmHg = 1333.22 Pa). A_g is the surface area in cm^2 g^{-1} of sorbent and v is the Gibbs excess uptake in cm^3 at s.t.p. g^{-1}. Values of the constants k_s for both carbons are given in table I. 1. These constants are not given where the limiting slopes as $v \to 0$ were difficult to obtain (Xe, CO_2, C_2H_6 and C_3H_8 on Carbolac) or where the isotherms were thought to be insufficiently accurate (Ne on Graphon). For the more condensable gases k_s was larger on Carbolac than on Graphon, but for the weakly sorbed H_2 k_s seems slightly larger on Graphon. In the temperature range covered the Henry law constants for D_2 and H_2 on Carbolac were numerically almost identical.

TABLE I. 1. THE HENRY LAW COEFFICIENTS, $k_s = C'_s/C'_g$ IN cm. VALUES GIVEN ARE $10^8\,k_s$

	gas									
T/K	H_2	D_2	Ne	Ar	Kr	Xe	N_2	CO	CH_4	C_2H_6
				(*a*) Carbolac carbon						
308.15	5.3_1	5.3_1	1.6_0	40.7	$192._1$	—	42.9	63.4	$177._7$	—
320.65	4.8_6	4.8_4	1.5_2	34.1	$142._9$	—	32.6	50.8	$132._2$	—
333.15	4.4_4	4.4_5	1.3_7	29.1	$114._1$	—	29.7	41.5	$105._4$	—
352.90	3.9_2	3.9_2	1.2_1	22.7	81.7	—	23.1	32.0	78.6	—
378.00	3.4_8	3.3_6	1.0_5	17.1	55.7	—	17.7	23.8	54.2	—
				(*b*) Graphon carbon						
308.15	5.8_6	—	—	29.2	80.1	$357._7$	32.1	—	77.0	$556._2$
320.65	5.4_4	—	—	25.8	68.2	$285._9$	28.0	—	65.5	$428._9$
333.15	5.0_9	—	—	23.1	58.8	$232._5$	24.8	—	56.4	$337._2$
343.15	4.8_3	—	—	21.3	52.7	$199._1$	22.6	—	50.3	$281._6$
353.15	4.6_1	—	—	19.7	47.4	$172._0$	20.7	—	45.3	$237._7$
363.15	4.4_1	—	—	18.2	43.0	$149._9$	19.0	—	41.0	$202._7$
373.15	4.2_2	—	—	17.0	39.1	$131._5$	17.6	—	37.3	$174._1$
393.15	3.9_0	—	—	14.9	32.9	$103._3$	15.2	—	31.3	$131._5$
S	0.2_4	—	—	0.5	0.8	3.0	0.3	—	0.8	$2._6$

All values of k_s for Graphon are smoothed and have been obtained by placing the best straight line through the experimental points in plots of $\lg Ak_s$ against K/T. Accordingly, the standard deviations, S, of experimental from smoothed values of k_s are included in table I. 1. As shown in an earlier analysis (Barrer & Rees 1961) k_s increases rapidly with those properties which reflect the condensability of the sorbates, such as boiling-point or polarizability.

I. 3.3. *Sorption heats and energies*

One may define an energy of adsorption, $\Delta E'$, by the relation

$$\Delta E' \equiv RT^2 \,\mathrm{d}\ln k_s/\mathrm{d}T. \tag{I. 2}$$

These energies are given in table I. 2. Although there are some variations the ratio of $\Delta E'$ for Carbolac to $\Delta E'$ for Graphon tends to increase as the $\Delta E'$ increase. This is most apparent for Ar, Kr and Xe, fully symmetrical molecules without permanent electric moments.

An isosteric heat, q'_{st}, may also be defined by the relation

$$RT^2\left(\frac{\partial \ln p}{\partial T}\right)_v \equiv q'_{st}. \tag{I. 3}$$

From equations (I. 1) and (I. 3) it is seen that

$$q'_{st} = -\Delta E' + RT. \qquad (I.4)$$

$\Delta E'$ for C_2H_6 and C_3H_8 in table I. 2 was derived, by using equation (I. 4), from q'_{st} as v, the amount adsorbed, tended to zero. The more condensable gases gave curved isotherms, as shown in figure I. 1, and q'_{st} was found for several of these gases, as a function of the amount sorbed, from plots of $\lg p$ against K/T for each of a series of values of v.

TABLE I. 2. ENERGIES OF ADSORPTION, $\Delta E'$/kJ mol^{-1} ON CARBOLAC AND GRAPHON

gas	$-\Delta E'$ Graphon	$-\Delta E'$ Carbolac	ratio of the $\Delta E'$
H_2	4.6	6.0	1.30
Ne	—	6.2	—
Ar	7.8	11.9	1.53
N_2	8.9	12.5	1.40
CO	—	13.9	—
Kr	10.5	16.9	1.61
CH_4	10.7	16.1	1.50
CO_2	—	25.6	—
Xe	14.7	26.2	1.78
C_2H_6	17.1	29.4	1.72
C_3H_8	22.1	39.0	1.76

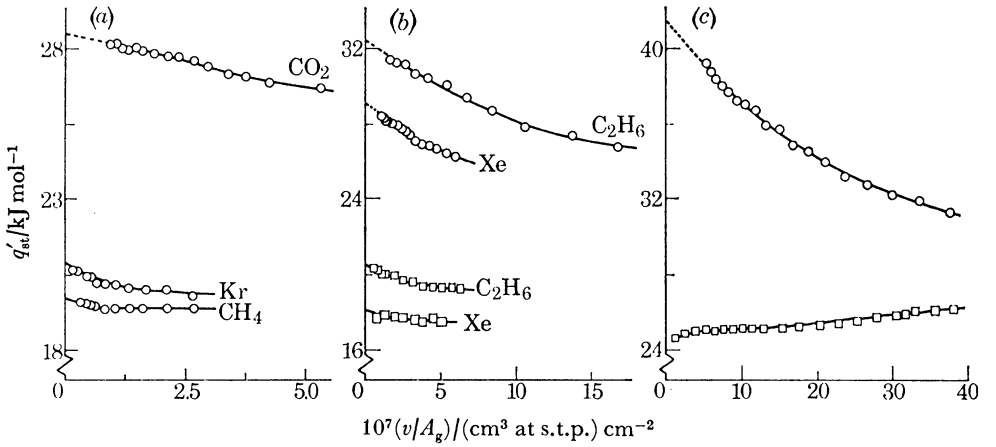

FIGURE I. 3. Isosteric heats (q'_{st}) as a function of coverage (v/A_g). (*a*) CO_2, Kr and CH_4 on Carbolac; (*b*) C_2H_6 and Xe on Carbolac and Graphon; (*c*) C_3H_8 on Carbolac and Graphon; ○, Carbolac; □, Graphon.

The heterogeneity of the carbon surfaces is seen from the decrease in q'_{st} with increasing v/A_g, the uptake per unit area of surface (figure I. 3). This is proportional to the fraction of monolayer coverage for a given gas and independent of the carbon. In the case of Carbolac when Henry's law was not obeyed the decrease in q'_{st} with increasing uptake did not level off at relatively high coverage. On Graphon when the Henry law was not obeyed (Xe, C_2H_6, C_3H_8), the initial q'_{st} was smaller than for the corresponding gas on Carbolac, the initial decrease with coverage was less steep and q'_{st} showed a more pronounced tendency to level off. This indicates a greater heterogeneity of Carbolac than Graphon. In the case of propane on Graphon q'_{st} tended to increase with coverage, due to the considerable exothermal interaction between pairs of adsorbed propane molecules. For a given sorbate the negative slope of curves of q'_{st} against uptake should depend on

temperature because as the temperature rises the molecules redistribute themselves among site groups. Eventually, in the Henry law range, the slope becomes zero because the populations of each site group obey the Henry law. Nevertheless, the redistribution should result in an increased temperature coefficient in q'_{st} or $\Delta E'$ as compared with a homogeneous sorbent (Barrer & Rees 1961).

I. 4. *Discussion*

I. 4.1. *Absolute and Gibbs excess adsorption*

If the sorbent–sorbate mixture is treated as a solution comprising n_s molecules of sorbate for a fixed amount of sorbent, then

$$\left(\frac{\partial p}{\partial T}\right)_{n_s} = \frac{\bar{H}_s - \tilde{H}_g}{T(\bar{V}_s - \tilde{V}_g)} = \frac{\Delta\bar{H}}{T(\bar{V}_s - \tilde{V}_g)}, \tag{I. 5}$$

which for a perfect gas leads to

$$RT^2\left(\frac{\partial \ln p}{\partial T}\right)_{n_s} \equiv q_{st} = -\frac{\Delta\bar{H}}{1 - \bar{V}_s/\tilde{V}_g}. \tag{I. 6}$$

In these relations $\bar{H}_s$ and $\tilde{H}_g$ are respectively the differential enthalpy per mole of sorbed molecules and the integral enthalpy per mole of gaseous molecules, while $\bar{V}_s$ and $\tilde{V}_g$ are the partial molar volume and molar volume of sorbed and gaseous molecules respectively. However, n_s in the sorbate–sorbent mixture is the total, or absolute, rather than the Gibbs excess uptake, n'_s. Thus, q_{st} is not the isosteric heat q'_{st} of equation I. 3, but is the isosteric heat for absolute adsorption.

The relation between q_{st} and q'_{st} is (Barrer & Papadopoulos 1972)

$$\frac{q'_{st}}{q_{st}} = \frac{(\partial n'_s/\partial T)_p\,(\partial n_s/\partial p)_T}{(\partial n_s/\partial T)_p\,(\partial n'_s/\partial p)_T}, \tag{I. 7}$$

and so depends upon the slopes of isobars and isotherms for absolute and the Gibbs excess sorptions. If the gas phase obeys the ideal gas law equation (I. 7) gives (Barrer & Papadopoulos 1972)

$$\frac{q'_{st}}{q_{st}} = \left\{1 + \frac{v_s}{RT}\left(\frac{\partial p}{\partial n'_s}\right)_T\right\} \Big/ \left\{1 - \frac{pv_s}{RT^2}\left(\frac{\partial T}{\partial n'_s}\right)_p\right\}, \tag{I. 8}$$

where v_s is the sorption volume available to adsorbed molecules in the mixture.

If the fixed amount of sorbent is taken to be a gram and the area per g is A_g, then $n'_s = A_g C'_s$ and $v_s/A_g = \delta$ where δ is the mean thickness of the sorption volume. By contrast with porous zeolite crystals v_s ($cm^3\,g^{-1}$) is not clearly definable. However, in the dilute Henry law range it will be assumed that δ is one molecular diameter with the proviso that $A_g\delta = v_s$ cannot exceed ϵ_g ($cm^3\,g^{-1}$), so that in this limit and thereafter $v_s = \epsilon_g$. Equation (I. 8) can be rearranged to

$$\frac{q'_{st}}{q_{st}} = \left[1 + \frac{\delta}{RT}\left(\frac{\partial p}{\partial C'_s}\right)_T\right] \Big/ \left[1 - \frac{p\delta}{RT^2}\left(\frac{\partial T}{\partial C'_s}\right)_p\right]. \tag{I.9}$$

Since in the Henry law range $(C'_s/T)\,(\partial T/\partial C'_s)_p$ can be shown to equal $-RT/q'_{st}$ it follows from equation (I. 9) that in this range

$$q_{st} = \frac{q'_{st}k_s + RT\delta}{k_s + \delta}, \quad \Delta E = \frac{\Delta E' k_s}{k_s + \delta}. \tag{I. 10}$$

The ratio q'_{st}/q_{st} thus always exceeds unity but, especially since $q'_{st} > RT$, this ratio approaches unity when $k_s \gg \delta$.

Some values of ΔE, with δ equated to the molecular diameters of the respective sorbates, were found from equation (I. 10) and are given in table I. 3. The ratios $\Delta E'/\Delta E$ are close to unity, except for the very weakly adsorbed gases Ne and H_2.

I. 4.2. *Standard free energies and entropies for absolute adsorption*

The total or absolute number of molecules in the adsorption volume per unit area of surface is $C'_s + \delta C'_g$ and the total number per unit sorption volume is therefore $C'_s/\delta + C'_g$. In the Henry law range the dimensionless equilibrium constant K for absolute sorption is then given by

$$K = \left(\frac{C'_s}{\delta} + C'_g\right) \Big/ C'_g = \left(\frac{k_s}{\delta} + 1\right). \tag{I. 11}$$

TABLE I. 3. ESTIMATE OF $\Delta E = -q_{st} + RT$

gas	$10^8 \times$ molec. diam./cm	$10^8(k_s+\delta)$/cm at 308.15K		$-\Delta E$/kJ mol^{-1}		$\Delta E'/\Delta E$		ρ
		Carbolac	Graphon	Carbolac	Graphon	Carbolac	Graphon	
H_2	2.50	7.8	8.3_6	4.0_8	3.2_2	1.46	1.43	1.27
Ne	3.20	4.8_0	—	2.0_7	—	2.9_5	—	—
Ar	3.82	44.5	33.0	10.9	6.9	1.09	1.13	1.58
Kr	4.04	196.0	$84._1$	16.6	10.0	1.02	1.05	1.66
Xe	4.56	—	362.0	—	14.5	—	1.01	—
N_2	4.0	46.9	36.1	11.4	7.9	1.10	1.13	1.44
CH_4	4.29	182.0	$81._3$	15.7	10.1	1.03	1.06	1.55
C_2H_6	5.2	—	561.0	—	16.9	—	1.01	—

In this dilute range the activity coefficients of sorbed and gaseous molecules are each unity so that K is the thermodynamic equilibrium constant. If δ for each sorbate molecule is assumed independent of temperature equation (I. 11) shows that

$$\frac{\mathrm{d}\ln K}{\mathrm{d}T} = \frac{\mathrm{d}\ln(k_s+\delta)}{\mathrm{d}T},$$

so that $\Delta E = \Delta E^{\ominus}$, the standard heat of adsorption. One also has for the standard free energy, $\Delta A^{\ominus}$, and entropy, $\Delta S^{\ominus}$, the relations $\Delta A^{\ominus} = -RT\ln K$ and $\Delta S^{\ominus} = (\Delta E^{\ominus} - \Delta A^{\ominus})/T$. These quantities were each calculated at 308.15 K from equation (I. 11) and from the energies in table I. 3. Their values are given in table I. 4. $-\Delta S^{\ominus}$ is considerably larger on Carbolac than on Graphon surfaces, a difference which may be interpreted as follows.

If the adsorbed molecules were freely rotating (where rotation is involved) and, in addition, have two translational and one vibrational modes relative to the surface ($\Delta S^{\ominus}_{\mathrm{I}}$); or one translational and two vibrational modes ($\Delta S^{\ominus}_{\mathrm{II}}$); or three vibrational modes ($\Delta S^{\ominus}_{\mathrm{III}}$), then (Barrer & Rees 1961)

$$\Delta S^{\ominus}_{\mathrm{I}} = R\ln\left[\left(\frac{kT}{2\pi m}\right)^{\frac{1}{2}} \frac{e^{\frac{1}{2}}}{\nu\delta}\right] + \tfrac{1}{2}R \tag{I. 12}$$

and

$$\Delta S^{\ominus}_{\mathrm{I}} = \tfrac{1}{2}\Delta S^{\ominus}_{\mathrm{II}} = \tfrac{1}{3}\Delta S^{\ominus}_{\mathrm{III}}. \tag{I. 13}$$

In equation (I. 12) m is the mass of the sorbate molecule of diameter δ vibrating with a mean frequency ν. Values can be assigned to ν only upon a semi-empirical basis (Hill 1952) according to the relation

$$\frac{\nu_1}{\nu_2} = \sqrt{\frac{\Delta E'_1 m_2}{\Delta E'_2 m_1}}, \tag{I. 14}$$

where $\nu_2 = 1.0 \times 10^{12}\,s^{-1}$ when $\Delta E_2' = -6.27\,kJ\,mol^{-1}$ and m_2 is the mass of an argon atom. Calculations for Ar, Kr, Xe and CH_4 as examples then showed that on Carbolac all these molecules had entropies, $\Delta S^{\ominus}$, between those calculated from equations (I. 12), (I. 13) and (I. 14) for $\Delta S^{\ominus}_{II}$ and $\Delta S^{\ominus}_{III}$, while on Graphon $\Delta S^{\ominus}$ for the same gases lay between those calculated for $\Delta S^{\ominus}_{I}$ and $\Delta S^{\ominus}_{II}$. Thus on Graphon, according to this criterion, the adsorbed molecules are largely mobile, while on Carbolac they are in part behaving as oscillators. Such behaviour reflects the energetic heterogeneity and greater mean bonding energy between Carbolac and the sorbates. It also indicates one reason for the observed greater efficiency of Graphon than Carbolac, per unit area of surface, in generating extra fluxes when there is a concentration gradient of adsorbed molecules (Ash *et al.* 1967).

TABLE I.4. $\Delta A^{\ominus}$ AND $\Delta S^{\ominus}$ AT 308.15 K

	$-\Delta A^{\ominus}$/kJ mol^{-1}		$-\Delta S^{\ominus}$/J mol^{-1} K^{-1}	
gas	Carbolac	Graphon	Carbolac	Graphon
H_2	2.9_2	3.0_9	3.7_6	0.4
Ne	1.0_4	—	3.3_4	—
Ar	6.2_9	5.5_2	14.9	4.5
Kr	10.0	7.7_8	21.4	7.1
Xe	—	11.2	—	10.7
N_2	6.3_1	5.6_4	16.6	7.5
CH_4	9.6	7.5_4	19.8	8.4
C_2H_6	—	12.0	—	15.9

I. 4.3. *Correlations involving equilibria and energetics*

As noted earlier, the Henry law constants, k_s, increase rapidly with properties related to condensability and therefore so should the constant, K, for absolute sorption. The empirical relation between $\lg K$ and sorbate polarizability, α, is shown in figure I.4*a*, at 308.15 K. Comparatively smooth relations are observed such as appear also for solutions of non-polar gases in liquids (Saylor & Battino 1958). A linear relation was also found between $-\Delta E$ and α (figure I.4*b*) and therefore between $\lg K$ and $-\Delta E$ (figure I.4*c*). These relations further indicate that at any particular temperature $\Delta A^{\ominus}$ and $\Delta E^{\ominus}$ correlate in a linear manner and therefore that $\Delta S^{\ominus}$ is a linear function of $\Delta E^{\ominus}$ (figure I. 5). Such behaviour has been observed in other systems (Frank 1945; Everett 1950; Barrer & Rees 1959).

If the interaction between a sorbate atom and an atom of the sorbent is represented by a Lennard-Jones 6:12 potential and if all pair interactions are additive, then for an ideally plane surface of the adsorbent the total energy of interaction at the minimum of the energy–distance curve is (Young & Crowell 1962)

$$E = -\pi A_{12} N / 9 Z_0^3. \qquad \text{(I. 15)}$$

In obtaining equation (I. 15) summation of pair interaction has been replaced by integration. Z_0 is the perpendicular distance at the minimum of the potential energy well from the centre of the sorbate molecule to the plane which contains the centres of the first layer of atoms comprising the sorbent surface. A_{12} is the dispersion energy constant and N denotes the number of atoms of adsorbent per m^3 of this adsorbent. Z_0 is related to the sum, d_0, of the van der Waals radii r_1 and r_2 respectively of a carbon atom and of the sorbate molecule by

$$Z_0 = 0.765 d_0 = 0.765(r_1 + r_2). \qquad \text{(I. 16)}$$

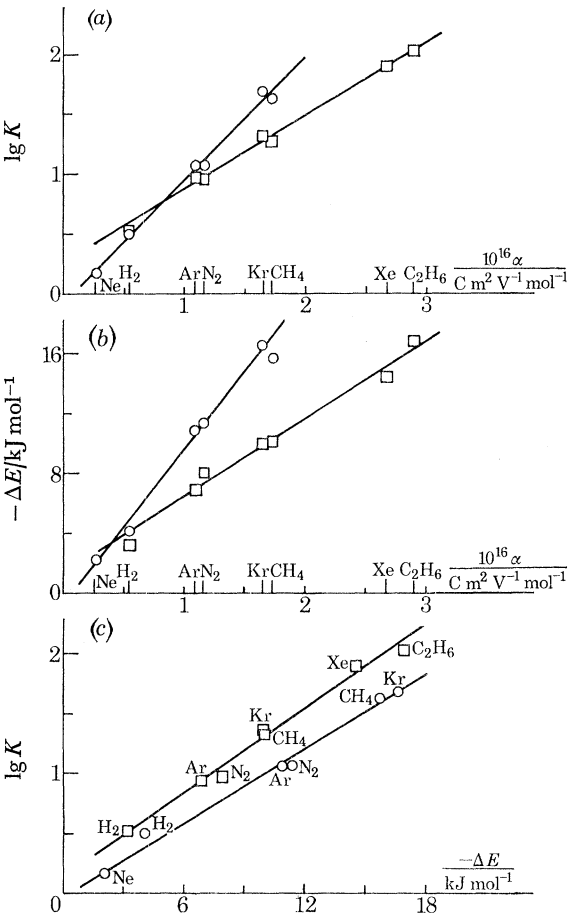

FIGURE I. 4. Relations between K, α and $-\Delta E$ for various gases on Carbolac and Graphon: (a) lg K against α; (b) $-\Delta E$ against α; (c) lg K against $-\Delta E$. ○, Carbolac; □, Graphon.

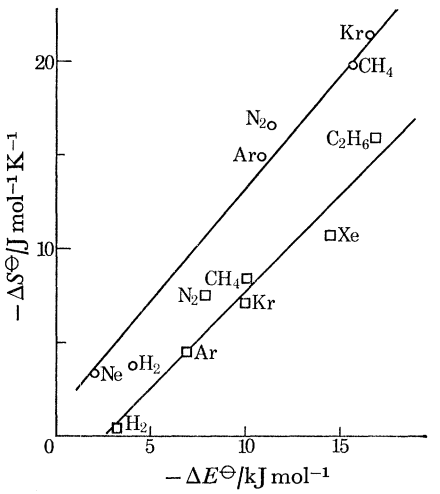

FIGURE I. 5. The relation between $-\Delta S^{\ominus}$ and $-\Delta E^{\ominus}$ for various sorbates on Carbolac, ○, and Graphon, □.

The value of E at the equilibrium distance Z_0 less the zero-point energy, E_0, is the energy of adsorption ΔE_0 at absolute zero provided dispersion and close range repulsion energies dominate. At higher temperatures molecules will have more vibrational energy than corresponds with E_0, but ΔE_0 should remain a good approximation to the values of ΔE given in table I. 4 for total or absolute adsorption. This means that the quotient $\Delta E Z_0^3/A_{12}$ should be approximately constant for a series of gases on ideally smooth surfaces. According to the three expressions for A_{12} due to London (1930), Slater & Kirkwood (1931) and Kirkwood and Müller (Kirkwood 1932; Müller 1936), one should thus have

$$\left.\begin{aligned}
\frac{-\Delta E Z_0^3\left(\frac{1}{E_1}+\frac{1}{E_2}\right)}{\alpha_2}\,\frac{32\pi^2\epsilon_0^2}{3\alpha_1} &= \text{constant} = R_1,\\
\frac{-\Delta E Z_0^3\left\{\left(\frac{\alpha_1}{n_1}\right)^{\frac{1}{2}}+\left(\frac{\alpha_2}{n_2}\right)^{\frac{1}{2}}\right\}}{\alpha_2}\,\frac{64\pi^3\sqrt{m}\,\epsilon_0^2}{3eh\alpha_1} &= \text{constant} = R_2,\\
\frac{+\Delta E Z_0^3\left(\frac{\alpha_1}{\chi_1}+\frac{\alpha_2}{\chi_2}\right)}{\alpha_2}\,\frac{8\pi^2\epsilon_0}{3mc^2\alpha_1} &= \text{constant} = R_3.
\end{aligned}\right\} \qquad \text{(I. 17)}$$

In these expressions α_1, α_2 and χ_1, χ_2 are respectively polarizabilities and diamagnetic susceptibilities of sorbent and sorbate. E_1 and E_2 are characteristic energies close to the ionization potentials, I_1 and I_2, of sorbent and sorbate and n_1 and n_2 are the corresponding numbers of electrons in the outermost completed electronic shells. m and e are the electronic mass and charge, h is the Planck constant, ϵ_0 is the permittivity of a vacuum and c the velocity of light. Numerical values of relevant constants are given in table I. 5.

TABLE I. 5. PHYSICAL CONSTANTS USED IN EVALUATION OF A_{12} AND E

	property				
atom or molecule	$10^{16}\alpha$ / C m² V⁻¹ mol⁻¹	$-10^{10}\chi$ / m³ mol⁻¹	assumed value of n	$10^{18}I$ / J (molecule)⁻¹	Z_0 / nm
H_2	0.538	0.50	2	2.63	0.224
Ne	0.263	0.85	8	3.46	0.250
Ar	1.090	2.45	8	2.53	0.274
Kr	1.647	3.52	18	2.24	0.283
Xe	2.681	5.41	18	1.94	0.302
N_2	1.162	1.51	10	2.50	0.281
CH_4	1.73	2.19	8	2.10	0.292
C_2H_6	2.900	3.44	14	2.05	0.327
CO_2	1.739	2.64	16	2.21	0.300
C	0.684	2.87	8	1.80	—

When the values of R_1, R_2 and R_3 for spherically symmetrical molecules were plotted against $-\Delta E$ the curves in figures I. 6*a* and *b* were obtained. For the heterogeneous Carbolac these coefficients increase several fold in our range in ΔE, but for Graphon the dependence on $-\Delta E$ is much smaller and so more nearly in line with the relations (I. 17). This difference in behaviour we associate with the heterogeneity of the Carbolac surfaces. Thus, in crevices and fissures on a sufficiently fine scale the assumption of plane surfaces of great extent, used in deriving equations (I. 15) and (I. 16), is not met. Indeed in crevices of molecular dimensions the E's may become

specific functions of the dimensions of particular molecules relative to those of the crevices (de Boer & Custers 1934). The roughness factor of Carbolac may be seen from the B.E.T. area of the free powder and the smoothed area estimated with the electron microscope. These have been reported as 950 and 264 $m^2 g^{-1}$ respectively (G. L. Cabot Ltd, data sheets).

By contrast with Carbolac, the more oxygen free surface, smoother surface texture and better crystallinity of Graphon evidently ensures that equations (I. 15) and (I. 16) are more reasonable approximations. Only parameters of the carbon atom and of adsorbate molecules have been used to evaluate A_{12}. Thus the dependence of the ratios R_1, R_2 and R_3 upon ΔE may serve to investigate energetic heterogeneity in the Henry law range whether the heterogeneity is due to surface roughness or chemisorbed impurity. In using this method one should choose spherical molecules with zero permanent electric moments.

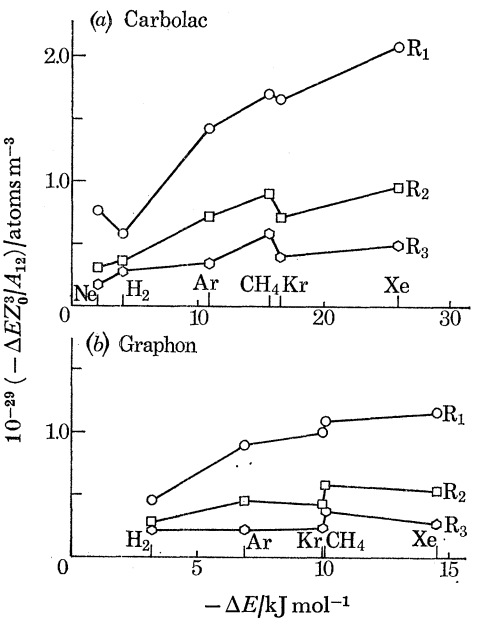

FIGURE I. 6. Variations of the ratios $-\Delta E Z_0^3/A_{12}$ with $-\Delta E$ for spherically symmetrical molecules with the use for A_{12} approximations due to London (○); Slater–Kirkwood (□) and Kirkwood–Müller (⬡). (*a*) Correlation for Carbolac; (*b*) correlation for Graphon.

I. 4.4. *Comparison of Graphon with Carbolac*

It will be assumed that Carbolac provides a homotattic surface with p groups of homogeneous sites, one of which, the first, relates to basal surfaces and is common to Carbolac and Graphon. The other groups in Carbolac relate to more energetically sorbing positions such as those in crevices. On Graphon it is assumed that the only site group contributing to adsorption is that comprising basal surfaces so that the Graphon surface is taken to be ideally homogeneous. For the jth site group on Carbolac one defines

$$\left.\begin{aligned} \phi_j &= \frac{(v_m)_j}{v_m} = \frac{\text{monolayer value for site group } j}{\text{monolayer value for whole surface}}, \\ \theta_j &= \frac{v_j}{(v_m)_j} = \frac{\text{amount adsorbed on site group } j}{\text{monolayer value for site group } j}. \end{aligned}\right\} \qquad \text{(I. 18)}$$

In the Henry law range one then has

$$\frac{\phi_j}{C_g} = \frac{h^3 a_j}{(2\pi mkT)^{\frac{3}{2}}} \exp(\zeta_j/kT), \tag{I. 19}$$

where a_j denotes the partition function for all motions of the adsorbed molecules relative to the surface and ζ_j is the least energy needed to move a molecule from the jth site group to the gas phase.

Site group 1 is the site group common to both carbons and on Graphon is the only site group. Therefore

$$\left.\begin{aligned} \theta_{1c} &= \theta_g, \quad \zeta_{1c} = \zeta_g, \\ a_{1c} &= a_g, \quad \phi_{1g} = \phi_g = 1, \end{aligned}\right\} \tag{I. 20}$$

where the subscripts c and g denote Carbolac and Graphon respectively. Thus for Carbolac

$$\theta_{jc} = \theta_g (a_{jc}/a_g) \exp[(\zeta_{jc} - \zeta_g)/kT]. \tag{I. 21}$$

The total fractional coverage θ_c of Carbolac is given by

$$\begin{aligned} \theta_c &= \sum_{j=1}^{p} (v_{jc}/v_{mc}) = \sum_{j=1}^{p} \theta_{jc}\phi_{jc} \\ &= \theta_g \left\{ \phi_{1c} + \sum_{j=2}^{p} \phi_{jc} (a_{jc}/a_g) \exp[(\zeta_{jc} - \zeta_g)/kT] \right\}, \end{aligned} \tag{I. 22}$$

if one makes use of the relations in equation (I. 20). Since

$$\sum_{j=1}^{p} \phi_{jc} = 1$$

it is obvious from equation (I.22) that θ_c/θ_g is > 1 or < 1 according respectively as

$$\sum_{j=2}^{p} \phi_{jc} (a_{jc}/a_g) \exp[(\zeta_{jc} - \zeta_g)/kT] > \text{ or } < \sum_{j=2}^{p} \phi_{jc}.$$

The terms a_{jc}/a_g contain the entropy contributions to θ_c/θ_g, while the exponentials provide the energy contributions. Thus for $\theta_c > \theta_g$ the energy contributions exceed those from the entropy, a situation met for all the sorbates of table I. 1 for which the comparison is possible save H_2.

For the adsorption energies, ΔE, the proportionality between K and θ/C_g requires, provided the monolayer saturation values v_{mc} and v_{mg} do not change with temperature, that

$$\Delta E_c = \Delta E_g + RT^2 \frac{\mathrm{d} \ln \eta}{\mathrm{d}T}, \tag{I. 23}$$

where

$$\eta = \left[\phi_{1c} + \sum_{j=2}^{p} \phi_{jc} (a_{jc}/a_g) \exp\{(\zeta_{jc} - \zeta_g)/kT\} \right].$$

Since $\zeta_{jc} > \zeta_g$, each being positive, the temperature coefficient $\mathrm{d} \ln \eta / \mathrm{d}T$ should be dominated by the exponentials in $1/T$ and so should be negative. Because the ΔE are negative, ΔE_c should then, as observed, be more exothermal than ΔE_g (table I. 3).

If one considers two gases, 1 and 2, of which 2 is more exothermally adsorbed than 1, then

$$\left.\begin{aligned} \rho_1 &= \frac{\Delta E_{1c}}{\Delta E_{1g}} = 1 + \frac{RT^2}{\Delta E_{1g}} \frac{\mathrm{d} \ln \eta_1}{\mathrm{d}T}, \\ \rho_2 &= \frac{\Delta E_{2c}}{\Delta E_{2g}} = 1 + \frac{RT^2}{\Delta E_{2g}} \frac{\mathrm{d} \ln \eta_2}{\mathrm{d}T}. \end{aligned}\right\} \tag{I. 24}$$

Thus at a common temperature T, ρ_2/ρ_1 is > 1 or < 1 according as $(1/\Delta E_{2g})\,(\mathrm{d}\ln\eta_2/\mathrm{d}T)$ exceeds or is less than $(1/\Delta E_{1g})\,(\mathrm{d}\ln\eta_1/\mathrm{d}T)$. The values of ρ in the last column of table I. 3 suggest that the first of these conditions is usually fulfilled since ρ tends to increase with increasing exothermicity of adsorption.

II. Isothermal flow

II. 1. *Introduction*

Studies of the extra flow in porous media arising from the presence of adsorbed films have been concerned both with dilute films, often obeying the Henry law, and with regions of high surface concentration up to and beyond monolayer coverage. Even when conditions are such that the surface concentration at the ingoing side of a high area microporous membrane is less than 0.05 of a saturated monolayer, the ratio of the extra flow to the flow expected in absence of adsorption may exceed 3 to 1 (Barrer & Strachan 1955). A random-walk diffusive mechanism has been found to describe the extra flow in the dilute film region (Aylmore & Barrer 1966), whereas hydrodynamic transport could occur at higher surface coverages (Gilliland, Baddour & Russell 1958; Barrer 1963).

In previous studies from these laboratories isothermal flows have been measured and interpreted for a number of microporous membranes, some of which have been composed of Carbolac carbon (Barrer & Strachan 1955; Ash *et al.* 1963*a*, *b*; Aylmore & Barrer 1966) and to a lesser extent of Black Pearls and Graphon carbons (Ash *et al.* 1967; Ash, Barrer & Lowson 1970). The energetically heterogeneous Carbolac surface and the large degree of energetic homogeneity of Graphon, discussed in part I, indicates that a fuller comparison of isothermal transport, using Carbolac and Graphon carbon membranes of comparable porosity, is of interest. The study complements an earlier investigation (Ash *et al.* 1967) and, with the equilibrium adsorption measurements on the membrane-forming carbons presented in part I, provides information needed for discussing and interpreting the thermo-osmotic transport reported in part III.

II. 2. *Experimental*

The gases studied were those used in part I.

The design of the apparatus followed that described elsewhere (Barrer & Gabor 1959), except that the plug assembly was constructed to enable isothermal or linear temperature gradient conditions to be imposed upon the porous medium. The membranes were made by compressing a number of approximately equal increments of carbon powder in stainless steel tubes with close-fitting hardened steel plungers. Pressures of approximately 25 ton/in^2 (1.54×10^7 Pa) were employed. After each addition the powder was compressed until the average porosity (void volume per unit volume) of the membrane formed up to that stage had reached a predetermined constant value. The lengths of successive stages of the membranes thus made were found by measuring the separation of the extremities of the plungers. After any loose material at the ends of the membrane had been brushed away, the membrane and holder were weighed to determine the weight of the membrane before outgassing. Stainless steel screw-in plungers of the type used by Carman & Malherbe (1950) and Ash *et al.* (1963*a*, *b*) were then fitted to prevent swelling of the membrane by the more strongly sorbed gases.

During outgassing at temperatures rising to 200 °C, as described in part I, the weight loss from

Carbolac, a separate sample being compressed in the same way as the membranes, was found to be 9.4 % (cf. 9 % of Carman & Raal (1951) and 9.3 % of Ash *et al.* (1963*a*, *b*)). The Graphon did not change appreciably in weight. The porosity calculations were based upon a value of 2.12 g cm^{-3} for the density of outgassed Carbolac as determined by Barrer & Strachan (1955). This compares with the value 2.13 g cm^{-3} of Rossman & Smith (1943). The value 1.97 g cm^{-3} was taken for the density of Graphon (G. L. Cabot Ltd., data sheets). The compacted Carbolac had a B.E.T. area of 940 m^2 g^{-1} and the compacted Graphon an area of 79 m^2 g^{-1} (part I). Relevant information concerning the three membranes is given in table II. 1.

TABLE II. 1. CHARACTERISTICS OF THE MICROPOROUS MEMBRANES

membrane†	material	estimated outgassed weight/g	no. of packing increments	length / cm	cross-sectional area/cm^2	porosity, ϵ / cm^3 cm^{-3}	area, A / m^2 cm^{-3}	ϵ/A / nm
L	Carbolac	1.416	6	4.05	0.320	0.484	1028	0.471
M	Carbolac	1.495	6	4.16	0.321	0.472	1052	0.449
N	Graphon	1.551	8	4.21	0.324	0.423	89.8_8	4.71

† Designated thus with reference to Ash *et al.* (1968).

A constant pressure of gas was maintained at the ingoing face of the membrane. The flow-rate was obtained by measuring the rate of increase of pressure in a calibrated volume at the outgoing side of the membrane. In order that this pressure could be ignored in comparison with the ingoing pressure, the former was never allowed to exceed 0.5 % of the latter. This requirement governed the choice of buffer volumes for the outgoing side. Thus, the boundary conditions for the isothermal flows were:

$$C(0, t) = C_0 = \text{constant}, \quad t > 0,$$

$$C(l, t) = C_l(t), \quad t > 0, \text{ where } C_i \ll C_0,$$

$$C(x, 0) = 0, \quad 0 < x < l.$$

In these relations, t denotes time and the membrane is bounded by the planes $x = 0$ and $x = l$. Flow is in the direction of x-increasing and C denotes the total concentration of diffusant, both adsorbed and in the gas phase, per cm^3 of porous medium. Subscripts 0 and l denote values at $x = 0$ and $x = l$ respectively.

The steady-state flow rate, G (J s^{-1}), was determined in each case from the relation

$$G = \frac{\mathrm{d}(pV)}{\mathrm{d}t}\frac{T}{T_\mathrm{R}} \text{ J s}^{-1}, \tag{II. 1}$$

where V (m^3) denotes the receiving volume at the outgoing side ($x = l$) in which the pressure at time t (s) is p (Pa) and T, T_R (Kelvin), are the membrane and room temperature respectively. The flow rate, G, is thus referred to the temperature of the membrane. A permeability, K (m^2 s^{-1}), may be defined by

$$K = Gl/A_\mathrm{c}\,\Delta p = Jl/A_\mathrm{c}\,\Delta C'_\mathrm{g}, \tag{II. 2}$$

where A_c (m^2) is the cross-sectional area normal to the direction of flow, Δp (Pa) is the pressure drop across the membrane of thickness l (m), J is the flux given in molecules per second and $\Delta C'_\mathrm{g}$ is the concentration drop in the gas phase (molecules m^{-3}) between the faces $x = 0$ and $x = l$.

It was, however, a matter of experimental convenience to measure p in cmHg, t in minutes and

relevant lengths, areas and volumes in cm, cm^2 and cm^3 respectively. Further, the permeability, K, is usually given in $cm^2\,s^{-1}$. With these modifications and all remaining quantities in the units already stated, we obtain as working equations for G and K:

$$\left.\begin{aligned} 10^7 G &= V\frac{dp}{dt}\frac{981\times 13.54}{60}\frac{T}{T_R}, \\ K &= V\frac{l}{A_c}\frac{dp}{dt}\frac{1}{60}\frac{1}{\Delta p}\frac{T}{T_R}. \end{aligned}\right\} \qquad \text{(II. 3)}$$

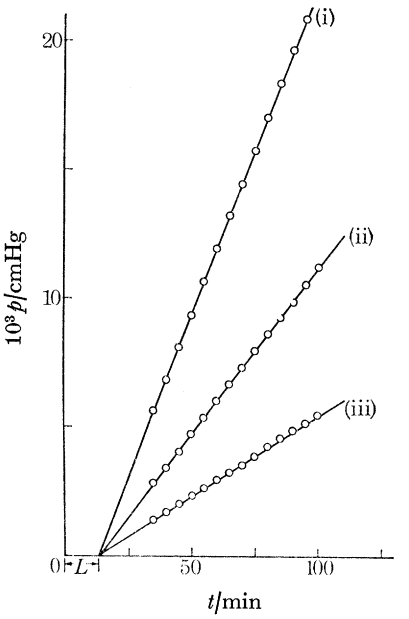

FIGURE II. 1. Outgoing pressure as a function of time; and time-lag, L, in typical permeability runs for Xe in membrane N at 308.15 K: p_0 = (i) 20 cmHg; (ii) 10 cmHg; (iii) 5 cmHg.

For the boundary conditions already given, figure II. 1 illustrates the change of pressure with time in the receiving volume, V, in this instance for xenon flowing through the Graphon membrane N. Extrapolation of the linear portion of the curves of p against t to cut the axis of time then gives the time-lags, L, which in this system are independent of the ingoing pressure p_0.

II. 3. *Results and discussion*

II. 3.1. *Permeabilities and time-lags*

Values of L and K for various systems for which K did not vary appreciably with ingoing pressure are shown in tables II. 2 and II. 3. For most of the systems L was also rather insensitive to pressure because adsorption was usually in or near the Henry law range. An exception is provided by Xe in Carbolac where both K and L show dependences on pressure arising from the strong curvature of the isotherms (part I). L will always depend upon ingoing pressure when adsorption is outside the Henry law range and in this respect is much more sensitive to pressure than K. For Xe in Carbolac L, L and K refer to mean values in the pressure range 10 to 30 cmHg.

In the absence of measurable 'surface' flow of deuterium one expects $K_{D_2} = K_{He}$ and in the absence of appreciable adsorption $L_{D_2} = L_{He}$. For the high area Carbolac surfaces K_{D_2}/K_{He} is *ca.* 1.4 and L_{D_2} is considerably larger than L_{He}. Thus both extra flow and adsorption of D_2 are

TABLE II. 2. TIME-LAGS AND PERMEABILITIES FOR CARBOLAC MEMBRANES

gas	T/K	L/min	$10^3\,K$/cm^2 s^{-1}	K_s/K_g	$10^3\,K_g$/cm^2 s^{-1}
		(*a*) membrane L			
He	308.15	(15.1_0)†	(0.973)†	—	—
	320.65	$15.1\ (14.8_1)$	$0.99_5\ (0.993)$	—	—
	333.15	$14.5\ (14.5_3)$	$1.01\ (1.01)$	—	—
	352.90	$14.1\ (14.1_1)$	$1.04\ (1.04)$	—	—
	378.00	$13.4\ (13.6_4)$	$1.08\ (1.08)$	—	—
Ne	308.15	39.7	0.52_8	0.21_6	0.43_4
	320.65	38.6	0.53_2	0.20_1	0.44_3
	333.15	36.9	0.53_8	0.19_6	0.45_0
	352.90	34.9	0.54_5	0.17_7	0.46_3
	378.00	32.7	0.55_7	0.15_8	0.48_1
Ar	308.15	$220._7$	0.82_0	1.6_5	0.30_9
	320.65	$192._4$	0.79_6	1.5_3	0.31_5
	333.15	$167._1$	0.76_9	1.4_0	0.32_0
	352.90	$140._0$	$0\ 74_3$	1.2_6	0.32_9
	378.00	$113._7$	0.72_9	1.1_3	0.34_2
Kr	308.15	—	0.91_0	3.2_7	0.21_3
	320.65	—	0.86_5	2.9_9	0.21_7
	333.15	—	0.82_2	2.7_2	0.22_1
	352.90	—	0.76_1	2.3_5	0.22_7
	378.00	348§	0.69_9	1.9_6	0.23_6
Xe	308.15	2706§	1.59	8.3_5	0.17_0
	320.65	—	1.44	7.2_8	0.17_4
	333.15	—	1.27	6.2_2	0.17_6
	352.90	—	1.16	5.3_7	0.18_2
	378.00	1266§	0.97_6	4.1_9	0.18_8
H_2	308.15	17.7	1.92	0.40	1.37
	320.65	16.8	1.92	0.37	1.40
	333.15	16.2	1.94	0.36	1.42
	352.90	15.0	1.95	0.33	1.46
	378.00	13.4	1.97	0.30	1.52
D_2	308.15	24.8	1.39	0.43	0.97_3
	320.65	23.6	1.40	0.41	0.99_3
	333.15	22.6	1.41	0.40	1.01
	352.90	21.0	1.42	0.37	1.04
	378.00	19.2	1.43	0.32	1.08
N_2	308.15	$203._8$	0.96_5	1.62	0.36_9
	320.65	$171._3$	0.91_9	1.44	0.37_6
	333.15	$151._4$	0.89_3	1.33	0.38_2
	352.90	$125._1$	0.85_7	1.17	0.39_3
	378.00	$102._5$	0.83_4	1.04	0.40_8
CO	320.65	$221._1$	1.04	1.77	0.37_6
	333.15	$184._1$	0.99_6	1.59	0.38_2
	352.90	$152._1$	0.94_8	1.40	0.39_3
	378.00	$123._0$	0.92_1	1.26	0.40_8
		(*b*) membrane M			
He	308.15	$18.8\ (18.5_1)$‡	$0.95_6\ (0.952)$‡	—	—
	320.65	$18.4\ (18.1_4)$	$0.97_2\ (0.971)$	—	—
	333.15	$17.5\ (17.8_0)$	$0.98_8\ (0.990)$	—	—
	352.90	$17.5\ (17.3_0)$	$1.02\ (1.02)$	—	—
	378.00	$16.3\ (16.7_1)$	$1.05\ (1.05)$	—	—
Kr	308.15	$915._0$	0.89_5	3.2_8	0.20_9
	320.65	$750._0$	0.84_1	2.9_7	0.21_2
	333.15	$624._0$	0.79_2	2.6_7	0.21_6
	352.90	$468._0$	0.72_6	2.2_6	0.22_3
	378.00	$365._7$	0.67_5	1.9_3	0.23_0
CO_2	308.15	1458.§	2.26	6.8_5	0.28_8
	320.65	—	2.03	5.9_3	0.29_3
	333.15	—	1.83	5.1_2	0.29_9
	352.90	—	1.59	4.1_6	0.30_8
	378.00	—	1.37	3.3_2	0.31_7
CH_4	308.15	$396._0$§	1.91	3.0_0	0.47_7
	320.65	—	1.81	2.7_4	0.48_4
	333.15	—	1.68	2.4_0	0.49_4
	352.90	—	1.56	2.0_6	0.50_9
	378.00	—	1.43	1.7_3	0.52_4
C_2H_6	333.15	—	3.31	8.1_7	0.36_1
	352.90	—	2.78	6.4_7	0.37_2
	378.00	—	2.36	5.1_6	0.38_3

† Smoothed values calculated from results at four temperatures by using the $\sqrt{T}$ relation.
‡ Smoothed values calculated from results at five temperatures by using the $\sqrt{T}$ relation.
§ Single run.

TABLE II.3. TIME-LAGS AND PERMEABILITIES FOR GRAPHON MEMBRANE N

gas	T/K	L/min	$10^2\,K$/cm^2 s^{-1}	K_s/K_g	$10^2\,K_s$/cm^2 s^{-1}	R
He	308.15	0.97 (0.91)†	1.60 (1.59)‡	—	—	—
	320.65	0.90 (0.89)	1.63 (1.63)	—	—	—
	333.15	0.88 (0.88)	1.67 (1.66)	—	—	—
	343.15	0.90 (0.86)	1.68 (1.68)	—	—	—
	353.15	0.80 (0.85)	1.71 (1.71)	—	—	—
	363.15	0.84 (0.84)	1.73 (1.73)	—	—	—
	373.15	0.66 (0.83)	1.75 (1.76)	—	—	—
	393.15	0.76 (0.81)	1.79 (1.80)	—	—	—
Ne	308.15	1.90	0.78_5	0.10_4	0.71_1	—
	320.65	1.81	0.79_5	0.10_1	0.72_2	—
	333.15	1.85	0.81_2	0.09_7	0.74_0	—
	343.15	1.74	0.82_0	0.09_6	0.74_8	—
	353.15	1.76	0.83_2	0.09_3	0.76_1	—
	363.15	1.71	0.84_2	0.09_1	0.77_2	—
	373.15	1.71	0.85_2	0.09_0	0.78_2	—
	393.15	1.67	0.86_9	0.08_6	0.80_0	—
Ar	308.15	2.94	0.81_6	0.62	0.50_5	$72._4$
	320.65	2.79	0.80_8	0.57	0.51_5	$72._5$
	333.15	2.63	0.80_4	0.53	0.52_5	$73._9$
	343.15	2.70	0.80_5	0.51	0.53_3	—
	353.15	2.50	0.80_0	0.48	0.54_1	—
	363.15	2.46	0.80_0	0.45	0.55_0	—
	373.15	2.39	0.79_8	0.44	0.55_6	—
	393.15	2.28	0.79_7	0.39	0.57_2	—
Kr	308.15	5.43	0.79_5	1.28	0.34_8	$76._9$
	320.65	4.96	0.77_3	1.18	0.35_5	$77._9$
	333.15	4.60	0.75_0	1.07	0.36_2	$78._2$
	343.15	4.38	0.73_6	1.01	0.36_7	—
	353.15	4.08	0.72_2	0.94	0.37_3	—
	363.15	3.88	0.71_2	0.88	0.37_8	—
	373.15	3.84	0.70_5	0.84	0.38_3	—
	393.15	3.55	0.69_2	0.76	0.39_4	—
Xe	308.15	13.0	1.08	2.91	0.27_6	$67._4$
	320.65	11.4	1.01	2.58	0.28_2	$69._9$
	333.15	9.87	0.94_3	2.27	0.28_8	$71._5$
	343.15	8.87	0.90_0	2.08	0.29_2	—
	353.15	8.16	0.87_2	1.95	0.29_6	—
	363.15	7.53	0.84_0	1.79	0.30_1	—
	373.15	6.99	0.81_2	1.66	0.30_5	—
	393.15	6.25	0.77_2	1.47	0.31_3	—
H_2	308.15	0.62	2.31	0.02_7	2.25	—
	320.65	0.63	2.36	0.03_1	2.29	—
	333.15	0.60	2.39	0.02_6	2.33	—
	343.15	0.57	2.42	0.02_5	2.36	—
	353.15	0.62	2.47	0.02_5	2.41	—
	363.15	0.63	2.50	0.02_0	2.45	—
	373.15	0.61	2.53	0.02_0	2.48	—
	393.15	0.57	2.59	0.02_0	2.54	—
D_2	308.15	0.86	1.65	0.03_8	1.59	—
	320.65	0.92	1.68	0.03_7	1.62	—
	333.15	0.90	1.71	0.03_6	1.65	—
	343.15	0.91	1.74	0.03_6	1.68	—
	353.15	0.88	1.76	0.03_5	1.70	—
	363.15	0.78	1.78	0.02_9	1.73	—
	373.15	0.84	1.81	0.02_8	1.76	—
	393.15	0.82	1.85	0.02_8	1.80	—
N_2	308.15	2.68	0.91_5	0.51	0.60_4	$62._1$
	320.65	2.55	0.91_1	0.48	0.61_5	$64._8$
	333.15	2.39	0.90_7	0.45	0.62_6	$65._4$
	343.15	2.34	0.90_4	0.42	0.63_6	—
	353.15	2.21	0.90_7	0.40	0.64_9	—
	363.15	2.18	0.90_5	0.38	0.65_5	—
	373.15	2.16	0.90_9	0.36	0.66_6	—
	393.15	1.99	0.91_1	0.34	0.67_9	—

† Smoothed values calculated from results at seven temperatures by using the $\sqrt{T}$ relation. Result at 373.15 K has been omitted.

‡ Smoothed values calculated from results at eight temperatures by using the $\sqrt{T}$ relation.

significant in Carbolac L. In Graphon N, however, K_{D_2} is, on average, only very slightly greater than K_{He} and L_{D_2} than L_{He}. In this membrane the gas permeability (measured with He) is however much larger than in Carbolac L, so that any contribution to K due to 'surface' permeability is less easy to detect. Also, the surface area is only about one-twelfth of that of Carbolac L so that the influence of adsorption upon L is also less easy to observe.

As adsorption increases the ratio of K for a given gas in Graphon N to K in Carbolac L decreases. Thus, for He this ratio is about 16 and for Xe about 7. The decrease is a result of the substantial adsorption of Xe (part I) and of the consequent extra flow associated with the mobile adsorbed layer having a concentration gradient.

For helium in both membranes the ratio $K/\sqrt{T}$ is independent of temperature. This suggests that transport of helium occurs only in the gas phase and, as expected in this work where the mean free paths of all gases were much greater than ϵ/A, that there is no viscous flow component in the gas phase. The observation supports the view that helium may be used as a non-sorbed calibrating gas (Ash *et al.* 1970). Time-lags for He in Graphon N are small and therefore are not very accurate. However, for a non-sorbed gas for which $K/\sqrt{T}$ does not depend on temperature, $L\sqrt{T}$ should also be independent of temperature. The mean value of $L\sqrt{T}$ was therefore found from results at each of seven temperatures, and the value of L calculated from this mean for each of the eight temperatures recorded in table II. 3. These are the values in brackets, which should be more accurate than the individual experimental values. They were subsequently used in estimates of 'surface' diffusion coefficients referred to later.

II. 3.2. *Component permeabilities*

The contribution to K which would be expected in absence of adsorption is termed K_g. This is readily obtained from the flow of helium, J_g^{He}, assuming the helium not to be adsorbed and that the adsorbed films do not block flow in the gas phase. The second component of K is termed K_s. It arises from the existence of mobile adsorbed films in a concentration gradient, and the extra flux, J_s, which results. One then has

$$K = K_s + K_g \tag{II. 4}$$

and under our flow conditions at a given temperature

$$K_g = K_g^{He}\sqrt{(M_{He}/M)}; \quad K_g^{He} = K_{He}, \tag{II. 4a}$$

where the M are the relative molecular masses of the calibrating gas (He) and the second gas. In this way K_s and K_g were found and their ratios included in tables II. 2 and II. 3. With the definition of K given in equation (II. 2) each ratio K_s/K_g is also the ratio of the corresponding fluxes, J_s/J_g. Thus the ratios in the tables show that J_s is greater in Carbolac membrane L than J_g for all species save Ne, H_2 and D_2. For these three gases K_s is the small difference between two large quantities, K and K_g, and so K_s is here uncertain. In Carbolac L, where K_s for these three gases is more accurate, the ratio K_s/K_g is very similar for H_2 and D_2, and for each of these two gases K_s/K_g exceeds the value for Ne.

Although K_s/K_g is smaller for a given gas on Graphon than on Carbolac, the extra flux generated per unit of available surface is much larger on Graphon as may be seen by evaluating the ratio

$$R = (K_s/A)_g\,(A/K_s)_c \tag{II. 5}$$

at several temperatures. The subscripts g and c here denote Graphon and Carbolac respectively.

The last column of table II. 3 shows this ratio for N_2, Ar, Kr and Xe. The behaviour confirms a previous report (Ash *et al.* 1967).

As already noted, except for Xe in Carbolac L, there is little dependence of K upon ingoing pressure for any of the gases in tables II. 2 and II. 3. However, for still more strongly adsorbed gases, K depended upon pressure to an extent which decreased with rising temperature and hence with diminishing adsorption. This behaviour is shown in figure II. 2 for C_3H_8 in Carbolac membrane M. An extreme example was found with Ar flowing through a Graphon membrane at 77.6 K where the low-pressure limit of K was more than 300 times its value at $p_0 = 20$ cmHg (Ash *et al.* 1967).

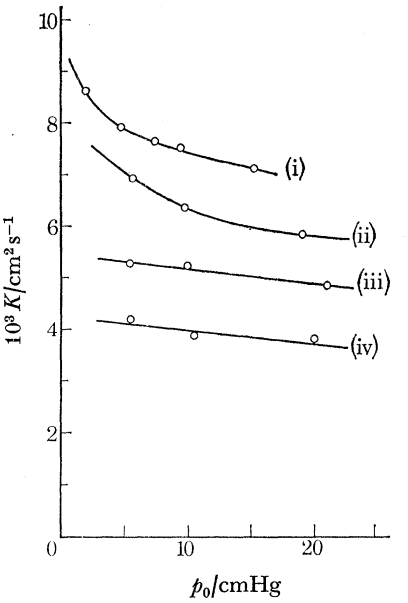

FIGURE II. 2. Dependence of permeability upon ingoing pressure for C_3H_8 in Carbolac membrane M. (i) 320.65 K; (ii) 333.15 K; (iii) 352.90 K; (iv) 378.00 K.

II. 3.3. *Relations between permeability coefficients and other properties of the gases*

In absence of a viscous component of flow in the gas phase and of extra flow J_s, $K(M/T)^{\frac{1}{2}}$ should be constant for a given membrane and series of non-sorbed gases. Departures from the value of $K(M/T)^{\frac{1}{2}}$ for helium can therefore be ascribed to J_s since, as noted earlier, there was in the membranes studied here no viscous component of gas phase flow. Values of $K(M/T)^{\frac{1}{2}}$ are plotted against T for several gases in figures II. 3 for Carbolac L and Graphon N. As temperature increases this quotient decreases, the more steeply the greater its value. Also the values of $K(M/T)^{\frac{1}{2}}$ for all gases fit upon a single curve when plotted against the Henry law adsorption constants k_s (given in part I) (figure II. 4*a*, *b*). A set of points was obtained for each gas in constructing these curves, one for each temperature at which K and k_s were measured. Figure II. 4 shows a good correlation between a kinetic and an equilibrium property. Similar correlations have been observed when, for a given membrane, $KM^{\frac{1}{2}}$ at constant T, or $K(M/T)^{\frac{1}{2}}$ is plotted against other properties which determine adsorbability. These include boiling point, T_B (Kammermeyer & Rutz 1959; Aylmore & Barrer 1966), energy of adsorption (Aylmore & Barrer 1966) and polarizability, α (Aylmore & Barrer 1966). All these correlations were equally clearly found in the

present work. It was further discovered that when $KM^{\frac{1}{2}}$ at constant temperature was plotted against the product αT_B the curves became the straight lines of figures II. 5*a*, *b*. Thus

$$KM^{\frac{1}{2}} = a(\alpha T_B) + b, \qquad \text{(II. 6)}$$

where a and b are constants at a given temperature. From such linear relations K may be estimated with reasonable accuracy for other simple molecules from the commonly known values of α and T_B. Graphs of $KM^{\frac{1}{2}}$ at constant temperature against α^2 and T_B^2 were also nearly linear, but in these cases the scatter was somewhat greater than in figure II. 5.

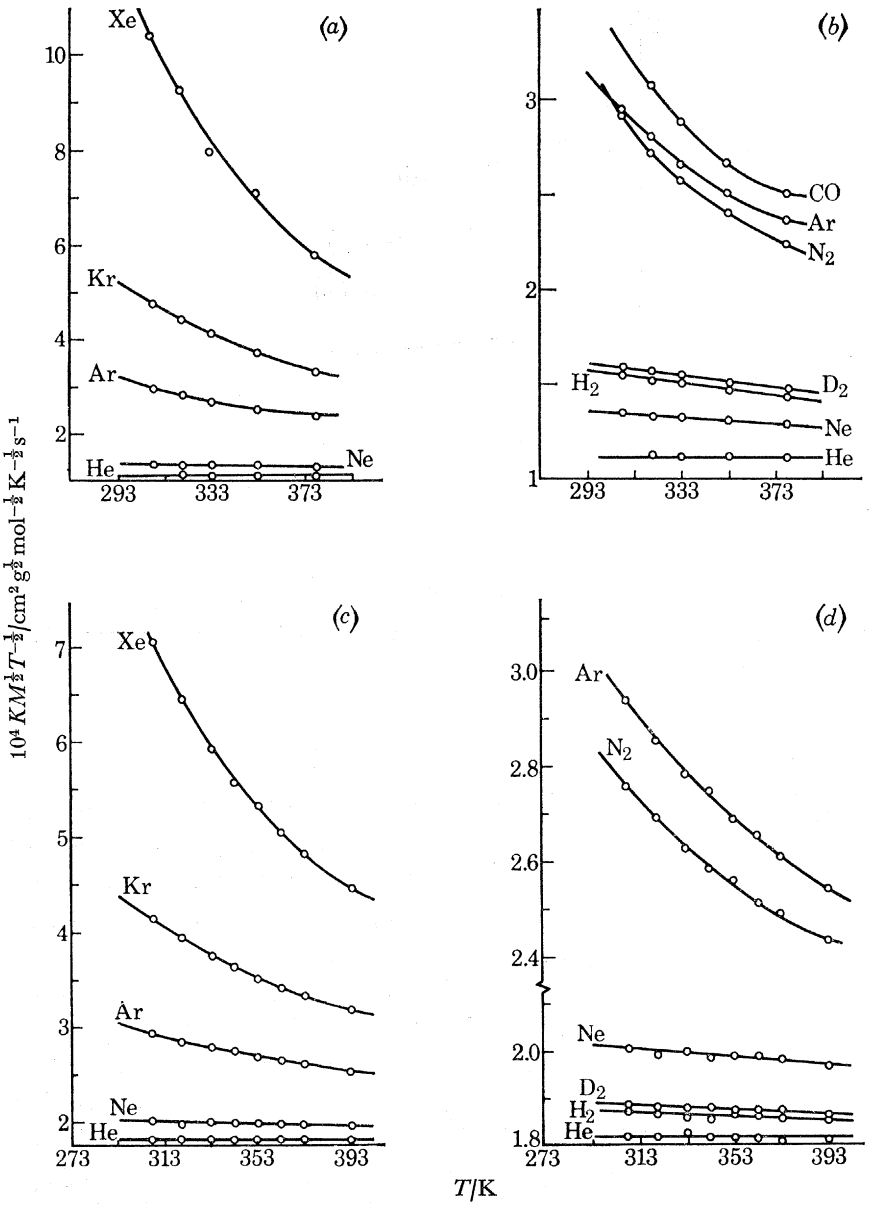

FIGURE II. 3. $K(M/T)^{\frac{1}{2}}$ as a function of temperature for a series of gases. (*a*), (*b*) Membrane L; (*c*), (*d*) membrane N.

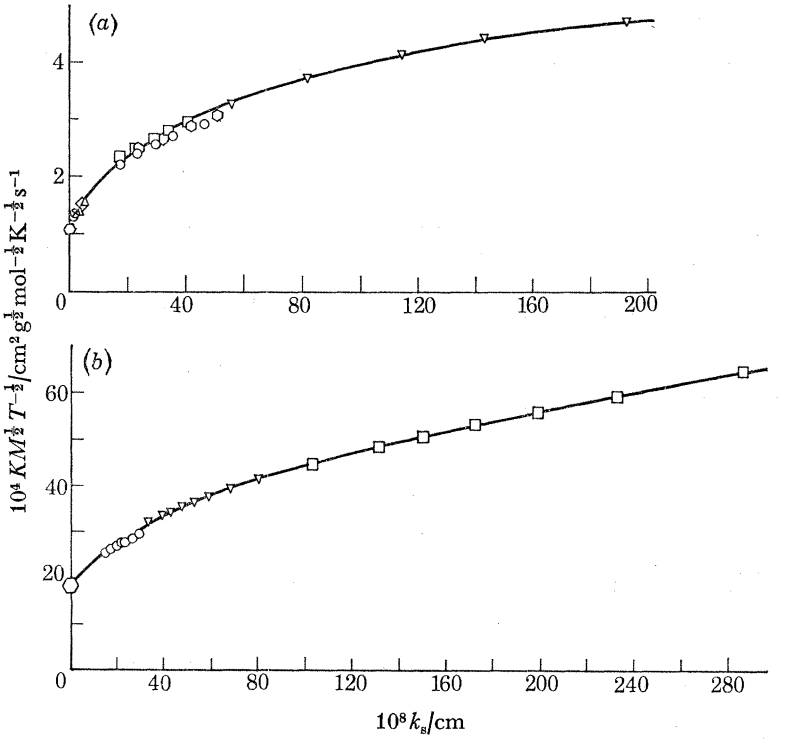

FIGURE II. 4. $K(M/T)^{\frac{1}{2}}$ as a function of the Henry law constant. (*a*) Membrane L: ⬡, He; ⊗, Ne; □, Ar; ▽, Kr; △, H_2; ◇, D_2; ○, N_2; ⬡, CO. (*b*) Membrane N: ⬡, He; ○, Ar; ▽, Kr; □, Xe.

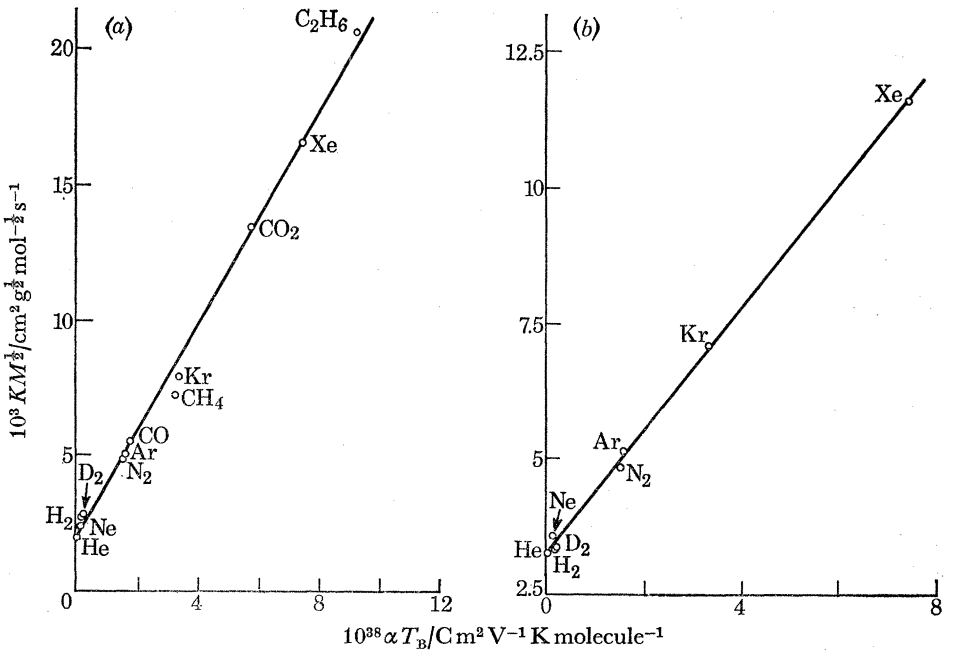

FIGURE II. 5. $KM^{\frac{1}{2}}$ at constant temperature as a function of αT_B. (*a*) Membrane L; (*b*) membrane N.

II. 3.4. *Diffusion coefficients*

In the Henry law range K_s and K_g in $K = K_s + K_g$ are given respectively by (Barrer & Gabor 1959)

$$K_s = D_{ss} A k_s; \quad K_g = D_{gs} \epsilon, \tag{II. 7}$$

where A and ϵ are area and pore volume per cm^3 of porous medium. The two diffusion coefficients D_{ss} and D_{gs} refer to the steady-state values of J_s and J_g respectively. The value of D_{gs} can be obtained from D_{gs} for helium at the same temperature according to equation (II. 8):

$$D_{gs} = D_{gs}^{He} \sqrt{(M_{He}/M)} = (K_g^{He}/\epsilon) \sqrt{(M_{He}/M)}. \tag{II. 8}$$

Thus equations (II. 7) and (II. 8) served to give D_{ss} and D_{gs} wherever k_s, A and K_g^{He} were known.

Also in the Henry law range the time-lag is given by (Barrer & Gabor 1960)

$$L = \frac{l^2(1 + Ak_s/\epsilon)}{6(D_g + D_s Ak_s/\epsilon)}, \tag{II. 9}$$

where D_g and D_s are diffusion coefficients for J_g and J_s respectively, characteristic of the transient flow during the establishment of the steady state. These coefficients are not necessarily identical with D_{gs} and D_{ss} because *inter alia* in the transient state all parts of the channel system must build up their final populations of adsorbed and gaseous molecules, while in the steady-state pores and crevices with blind-pore character will be wholly or partially bypassed. Their pore geometry and topography may differ from that of the through channels (Barrer & Gabor 1960). Again using helium as non-sorbed calibrating gas one has

$$D_g^{He} = l^2/6L_{He}; \quad D_g = D_g^{He} \sqrt{(M_{He}/M)}. \tag{II. 10}$$

Relations (II. 10) serve to give D_g. Also with the aid of equation (II. 10), equation (II. 9) may be rearranged to give

$$D_s = \frac{l^2}{6Ak_s/\epsilon} \left[\frac{1 + Ak_s/\epsilon}{L} - \frac{\sqrt{(M_{He}/M)}}{L_{He}} \right], \tag{II. 11}$$

so that D_s can also be obtained.

Values of the four diffusion coefficients are given in tables II. 4 and II. 5 for a number of gases in Carbolac L and M and Graphon N. Also given is the diffusion coefficient, D_g^{cyl}, which would be found for flow by molecular streaming in a single straight cylindrical capillary having a radius r identical with $2\epsilon/A$ for the porous medium (Barrer & Gabor 1959):

$$D_g^{cyl} = \frac{8}{3} \frac{\epsilon}{A} \sqrt{\frac{2RT}{\pi M}}. \tag{II. 12}$$

D_g^{cyl} serves as a reference value with which D_g and D_{gs} may be compared. In Graphon N each diffusion coefficient is an order of magnitude greater than its counterpart in Carbolac L. The ratios $D_g/D_g^{cyl} = \kappa_g$ and $D_{gs}/D_g^{cyl} = \kappa_{gs}$ define structure factors. These structure factors are < 1 when tortuosity and bottlenecks in the channel system are dominant and > 1 if through channels of greater-than-average dimensions tend to govern flow rates. From tables II. 4 and II. 5 the structure factors have the following values:

	Carbolac L	Carbolac M	Graphon N
κ_g	0.38	0.34	0.67
κ_{gs}	0.25	0.26	0.47

TABLE II.4. DIFFUSION COEFFICIENTS ($cm^2\ s^{-1}$) AND FLUX RATIOS FOR CARBOLAC MEMBRANES IN THE HENRY LAW RANGE

gas	property at T/K	T/K 308.15	320.65	333.15	352.90	378.00
		(*a*) membrane L				
H_2	$10^3 D_g^{cyl}$	11.3	11.5	11.7	12.1	12.5
	$10^3 D_g$	4.24	4.32	4.40	4.53	4.69
	$10^3 D_{gs}$	2.84	2.89	2.95	3.03	3.14
	$10^3 D_s$	1.10	1.19	1.31	1.57	1.71
	$10^3 D_{ss}$	1.00	1.04	1.12	1.20	1.26
	$D_s Ak_s/D_g\epsilon$	0.29	0.28	0.28	0.29	0.27
	Ak_s/ϵ	1.13	1.03	0.94_3	0.83_3	0.73_9
D_2	$10^3 D_g^{cyl}$	7.9_9	8.1_5	8.3_1	8.5_3	8.8_5
	$10^3 D_g$	3.00	3.06	3.11	3.20	3.32
	$10^3 D_{gs}$	2.01	2.05	2.08	2.15	2.22
	$10^3 D_s$	0.81	0.83	0.85	0.94	1.04
	$10^3 D_{ss}$	0.78	0.82	0.88	0.94	1.04
	$D_s Ak_s/D_g\epsilon$	0.31	0.28	0.26	0.24	0.22
	Ak_s/ϵ	1.13	1.03	0.94_5	0.83_3	0.70_9
N_2	$10^3 D_g^{cyl}$	3.03	3.09	3.15	3.24	3.35
	$10^3 D_g$	1.14	1.16	1.18	1.22	1.26
	$10^3 D_{gs}$	0.76	0.78	0.79	0.81	0.84
	$10^3 D_s$	0.121	0.147	0.162	0.188	0.229
	$10^3 D_{ss}$	0.136	0.150	0.166	0.193	0.228
	$D_s Ak_s/D_g\epsilon$	0.97	0.95	0.87	0.76	0.68
	Ak_s/ϵ	9.1_1	7.5_0	6.3_1	4.9_2	3.7_6
CO	$10^3 D_g^{cyl}$	—	3.09	3.15	3.24	3.36
	$10^3 D_g$	—	1.16	1.18	1.22	1.26
	$10^3 D_{gs}$	—	0.78	0.79	0.81	0.84
	$10^3 D_s$	—	0.118	0.141	0.165	0.195
	$10^3 D_{ss}$	—	0.127	0.144	0.168	0.209
	$D_s Ak_s/D_g\epsilon$	—	1.10	1.05	0.92	0.78
	Ak_s/ϵ	—	10.8	8.8_1	6.8_0	5.0_6
Ar	$10^3 D_g^{cyl}$	2.54	2.59	2.64	2.72	2.81
	$10^3 D_g$	0.95	0.97	0.99	1.02	1.05
	$10^3 D_{gs}$	0.64	0.65	0.66	0.68	0.71
	$10^3 D_s$	0.120	0.136	0.157	0.179	0.221
	$10^3 D_{ss}$	0.122	0.137	0.150	0.177	0.220
	$D_s Ak_s/D_g\epsilon$	1.09	1.01	0.98	0.85	0.76
	Ak_s/ϵ	8.6_5	7.2_4	6.1_8	4.8_2	3.6_3
Kr	$10^3 D^{cyl}$	1.75	1.79	1.82	1.88	1.94
	$10^3 D_g$	0.66	0.67	0.69	0.71	0.73
	$10^3 D_{gs}$	0.44	0.45	0.46	0.47	0.49
	$10^3 D_s$	—	—	—	—	0.080†
	$10^3 D_{ss}$	0.035	0.044	0.051	0.064	0.081
	$D_s Ak_s/D_g\epsilon$	—	—	—	—	1.32
	Ak_s/ϵ	40.8	30.4	24.2	17.4	11.8
		(*b*) membrane M				
He	$10^3 D_g^{cyl}$	7.6_5	7.8_0	7.9_5	8.1_8	8.4_7
	$10^3 D_g$	2.60	2.65	2.70	2.78	2.88
	$10^3 D_{gs}$	2.02	2.06	2.10	2.16	2.22
Kr	$10^3 D_g^{cyl}$	1.67	1.70	1.74	1.79	1.85
	$10^3 D_g$	0.57	0.58	0.59	0.61	0.63
	$10^3 D_{gs}$	0.44	0.45	0.46	0.47	0.49
	$10^3 D_s$	0.041	0.048	0.057	0.075	0.091
	$10^3 D_{ss}$	0.034	0.042	0.048	0.059	0.076
	$D_s Ak_s/D_g\epsilon$	3.06	2.64	2.45	2.25	1.80
	Ak_s/ϵ	42.8	31.9	25.4	18.2	12.4
CH_4	$10^3 D_g^{cyl}$	3.82	3.90	3.97	4.09	4.23
	$10^3 D_g$	1.30	1.32	1.35	1.39	1.44
	$10^3 D_{gs}$	1.01	1.03	1.05	1.08	1.11
	$10^3 D_s$	0.092†	—	—	—	—
	$10^3 D_{ss}$	0.077	0.095	0.107	0.127	0.159
	$D_s Ak_s/D_g\epsilon$	2.80	—	—	—	—
	Ak_s/ϵ	39.61	29.46	23.49	17.52	12.08

† Based upon a single run.

PHILOSOPHICAL TRANSACTIONS OF THE ROYAL SOCIETY A MATHEMATICAL, PHYSICAL & ENGINEERING SCIENCES

This indicates that in each membrane tortuosity and bottlenecks have the main influence and that this influence is more important in the steady state. A part in determining the κ must also be played by departures of the channels from the circular cross-section of the reference capillary of equation (II. 12).

TABLE II. 5. DIFFUSION COEFFICIENTS ($cm^2\ s^{-1}$) AND FLUX RATIOS FOR GRAPHON MEMBRANE N IN THE HENRY LAW RANGE

		T/K							
gas	property at T/K	308.15	320.65	333.15	343.15	353.15	363.15	373.15	393.15
H_2	$10^3 D_g^{cyl}$	113	115	$117._5$	119	121	$122._6$	124	$127._6$
	$10^3 D_g$	76.1	$77._6$	$79._0$	$80._2$	$81._4$	$82._6$	$83._7$	$85._9$
	$10^3 D_{gs}$	$53._3$	$54._3$	$55._6$	$56._0$	$57._0$	$57._6$	$58._3$	$59._6$
	Ak_s/ϵ	0.124	0.116	0.108	0.103	0.098	0.093	0.090	0.083
He	$10^3 D_g^{cyl}$	$80._2$	$81._8$	$83._4$	$84._6$	$85._8$	$87._0$	$88._2$	$90._6$
	$10^3 D_g$	$54._0$	$55._1$	$56._1$	$56._9$	$57._8$	$58._6$	$59._4$	$61._0$
	$10^3 D_{gs}$	$37._8$	$38._5$	$39._5$	$39._7$	$40._4$	$40._9$	$41._4$	$42._3$
Ne	$10^3 D_g^{cyl}$	$35._7$	$36._4$	$37._1$	$37._7$	$38._2$	$38._8$	$39._3$	$40._3$
	$10^3 D_g$	24.0	24.5	25.0	25.3	25.7	26.1	26.5	27.1
	$10^3 D_{gs}$	16.8	17.2	17.5	17.7	18.0	18.2	18.4	18.8
N_2	$10^3 D_g^{cyl}$	30.3	30.9	31.5	32.0	32.4	32.9	33.3	34.2
	$10^3 D_g$	20.4	20.8	21.2	21.5	21.8	22.2	22.5	23.0
	$10^3 D_{gs}$	14.3	14.6	14.9	15.0	15.3	15.5	15.6	16.0
	$10^3 D_s$	15.3	16.7	19.4	20.0	23.2	23.6	23.6	29.9
	$10^3 D_{ss}$	10.8	11.8	12.6	13.2	13.9	14.7	15.4	17.0
	$D_s Ak_s/D_g\epsilon$	0.51	0.48	0.48	0.45	0.47	0.43	0.39	0.42
	Ak_s/ϵ	0.68	0.60	0.53	0.48	0.44	0.40_3	0.37_4	0.32_3
Ar	$10^3 D_g^{cyl}$	25.3	25.9	26.4	26.8	27.2	27.6	27.9	28.7
	$10^3 D_g$	17.1	17.4	17.8	18.0	18.3	18.6	18.8	19.3
	$10^3 D_{gs}$	12.0	12.2	12.5	12.6	12.8	13.0	13.1	13.4
	$10^3 D_s$	16.2	18.0	20.6	18.7	23.0	23.7	25.5	28.8
	$10^3 D_{ss}$	11.9	12.7	13.5	14.2	14.6	15.3	15.9	16.8
	$D_s Ak_s/D_g\epsilon$	0.59	0.57	0.57	0.47	0.53	0.49	0.49	0.47
	Ak_s/ϵ	0.62	0.55	0.49	0.45	0.41_8	0.38_6	0.36_1	0.31_6
Kr	$10^3 D_g^{cyl}$	17.5	17.9	18.2	18.5	18.8	19.0	19.3	19.8
	$10^3 D_g$	11.8	12.0	12.3	12.4	12.6	12.8	13.0	13.3
	$10^3 D_{gs}$	8.3	8.4	8.6	8.7	8.8	8.9	9.0	9.2
	$10^3 D_s$	7.4	8.5	9.4	10.2	11.5	12.5	12.6	14.6
	$10^3 D_{ss}$	2.50	2.84	3.1_2	3.4_0	3.7_3	4.0_0	4.2_9	4.9_5
	$D_s Ak_s/D_g\epsilon$	1.07	1.02	0.96	0.91	0.91	0.89	0.81	0.77
	Ak_s/ϵ	1.70	1.45	1.25	1.12	1.01	0.91	0.83	0.70
Xe	$10^3 D_g^{cyl}$	14.0	14.3	14.6	14.8	15.0	15.2	15.4	15.8
	$10^3 D_g$	9.4	9.6	9.8	9.9	10.1	10.2	10.4	10.6
	$10^3 D_{gs}$	6.6	6.7	6.9	6.9	7.1	7.1	7.2	7.4
	$10^3 D_s$	3.0_4	3.4_4	4.0_1	4.5_1	4.9_2	5.3_7	5.8_4	6.6_1
	$10^3 D_{ss}$	2.50	2.84	3.12	3.4_0	3.7_3	4.0_0	4.2_9	4.9_5
	$D_s Ak_s/D_g\epsilon$	2.4_5	2.1_7	2.03	1.92	1.78	1.67	1.57	1.36
	Ak_s/ϵ	7.6	6.1	4.9_6	4.2_3	3.6_5	3.1_8	2.7_9	2.1_9

The ratios K_s/K_g given in tables II. 2 and II. 3 are, as noted earlier, also the ratios of J_s/J_g. The ratios $D_s Ak_s/D_g\epsilon$ (tables II. 4 and II. 5) are, for the transient state of the time-lag period, analogous to J_s/J_g for the steady state. In Carbolac L K_s/K_g always exceeds $D_s Ak_s/D_g\epsilon$, but in Carbolac M and Graphon N the two quotients are nearly equal. Ak_s/ϵ in tables II. 4 and II. 5 gives the ratios of the numbers of molecules present per cm^3 of porous medium in the adsorbed

film (as Gibbs excess uptakes) and the number which would be present in the gas phase, per cm^3 of medium, in absence of adsorption.

In Carbolac L for all the gases in table II. 4 $D_g/D_{gs} \sim 1.5$ and D_s/D_{ss} is close to unity, while for Kr and CH_4 in Carbolac M, $D_g/D_{gs} \sim 1.3$ and $D_s/D_{ss} \sim 1.2$. In Graphon N both D_g/D_{gs} and D_s/D_{ss} exceed unity. It is notable that whereas in Carbolac L and M D_s is always considerably smaller than D_g and D_{ss} than D_{gs}, in Graphon N, on the other hand, D_s and D_g or D_{ss} and D_{gs} are much closer in value. The above behaviour on Graphon is thought to be related in part to the greater surface uniformity of this carbon, so that translational freedom (part I) on this surface gives long surface mean free paths of mobile molecules. The non-uniformity and rougher texture

TABLE II. 6

(*a*) E_{ss} and D_{0s} in $D_{ss} = D_{0s} \exp(-E_{ss}/RT)$, and ratios $-E_{ss}/\Delta E'$

membrane	gas	E_{ss} / kJ mol^{-1}	$10^3 D_{0s}$ / cm^2 s^{-1}	$-E_{ss}/\Delta E'$
Carbolac L	Ne	3.3_1	2.0_1	0.54
	Ar	7.7_8, 8.1_8	2.5_4, 2.9_4	0.65, 0.69
	Kr	11.4_4	2.9_8	0.68
	Xe	17.6_6	6.6_1	0.67
	H_2	3.1_4	3.4_4	0.53
	D_2	3.9_6	3.6_4	0.63
	N_2	7.2_4	2.2_8	0.58
	CO	8.5_0	3.0_9	0.61
Carbolac M	Kr	11.1_3	2.6_1	0.66
	CO_2	15.9_8	10.3	0.62
	CH_4	10.5_9	4.6_1	0.66
Graphon N	Ar	4.2_3	62	0.54
	Kr	5.7_9	59	0.55
	Xe	8.1_1	59	0.55
	N_2	5.2_5	84	0.59

(*b*) E_s and D_0 in $D_s = D_0 \exp(-E_s/RT)$

		E_s / kJ mol^{-1}	$10^3 D_0$ / cm^2 s^{-1}
Carbolac L	Ar	8.3_4	3.1_1
	H_2	6.9_5	16.4_1
	N_2	8.5_8	3.5_8
	CO	8.7_4	3.2_2
Carbolac M	Kr	11.3_5	3.4_2
Graphon N	Ar	6.7_2	224
	Kr	8.1	178
	Xe	9.5	126
	N_2	7.2_5	260

of Carbolac surfaces gives less translational freedom and short surface mean free paths. A further important feature of the extra flow, J_s, is that through any cross-section a fraction of this extra flow (as measured with helium as non-sorbed calibrating gas) is in the gas phase because the molecules which comprise this flow must often evaporate in order to pass from one element of a broken surface to another, or from one carbon particle to another (Barrer & Gabor 1960). Accordingly, some of the mean free paths of the extra flow are always those appropriate to the gas phase. J_s has in the past been termed the surface flow, but this description is not an accurate one, since only part of J_s is in the surface.

II. 3.5. *Temperature dependence of D_{ss} and D_s*

The 'surface' diffusion coefficients gave approximately linear plots of lg D_{ss} or lg D_s against reciprocal temperature as found previously (Barrer & Gabor 1960). Thus one may write

$$D_{ss} = D_{0s}\exp(-E_{ss}/RT); \quad D_s = D_0\exp(-E_s/RT). \tag{II. 13}$$

Table II. 6 summarizes the values of E_{ss}, D_{0s}, E_s and D_0 for some of the gases. From the table it is seen that for a given molecule E_{ss} is less on Graphon than on Carbolac and that D_{0s} is much larger on the Graphon. The ratios $-E_{ss}/\Delta E'$ involve an energy of adsorption defined by

$$RT^2\,\mathrm{d}\ln k_s/\mathrm{d}T = \Delta E'.$$

$-E_{ss}/\Delta E'$ for each carbon is less than unity. The ratio would approach unity if the only energy barriers regulating the extra flow were those requiring complete evaporation across crevices or between particles of carbon. The observation that $-E_{ss}/\Delta E'$ is less than unity therefore indicates that other low-energy barriers in which the molecules comprising the extra flow are not desorbed also exercise an influence. The smaller E_{ss} and larger D_{0s} for Graphon are in accord with the greater energetic homogeneity and surface smoothness of this carbon as compared with Carbolac and also the greater hydraulic radius (ϵ/A) for Graphon. In Graphon N (table II. 6) E_s and D_0 in $D_s = D_0\exp(-E_s/RT)$ are both larger than E_{ss} and D_{0s}. For the Carbolac membranes these differences are much less pronounced (with the exception of the H_2 data for which the experimental error is greater).

Because of the physical meaning of J_s, direct comparisons of D_{ss} or D_s with theoretical models of surface diffusion for flows in which molecules comprising the flow never leave the surface are not appropriate. The significance of D_{ss} and E_{ss} (or D_s and E_s) in the composite flow J_s may be considered as follows. The extra flow J_s is divided into that part, J_s', which through any cross-section normal to x is entirely in the surface and that part $(J_s - J_s')$ in which the molecules are in the gas phase (Barrer & Gabor 1960). The corresponding diffusion coefficients are

$$D_1 = D_{01}\exp(-E_1/RT) \quad \text{and} \quad D_2 = D_{02}\exp(-E_2/RT).$$

Then
$$J_s = J_s' + (J_s - J_s') = -D_{ss}\,\mathrm{d}C_s/\mathrm{d}x = -D_1\,\mathrm{d}C_s/\mathrm{d}x - D_2\,\mathrm{d}C_s/\mathrm{d}x,$$

so that $D_{ss} = D_1 + D_2$. Accordingly

$$\frac{\mathrm{d}\ln D_{ss}}{\mathrm{d}T} = \frac{E_{ss}}{RT^2} = \frac{\mathrm{d}}{\mathrm{d}T}\{\ln[D_{01}\exp(-E_1/RT) + D_{02}\exp(-E_2/RT)]\}. \tag{II. 14}$$

In terms of the transition state formulation of diffusion (Glasstone, Laidler & Eyring 1941) the Arrhenius energy of activation, E, and the enthalpy and volume changes on activation, $\Delta H^\ddagger$ and $\Delta V^\ddagger$ respectively, are related by

$$E = RT + \Delta H^\ddagger - p\Delta V^\ddagger. \tag{II. 15}$$

For the molecules comprising J_s', which hop only along the surface, $p\Delta V^\ddagger$ is small and so $E_1 \simeq RT + \Delta H^\ddagger$. For the molecules comprising $(J_s - J_s')$, however, since they are activated from the condensed adsorbed phase into the gas phase, $p\Delta V^\ddagger \simeq RT$ and so $E_2 \simeq \Delta H^\ddagger = -\Delta H$, the heat of desorption. From the right-hand side of equation (II. 14) one sees that plots of ln D_{ss} (or ln D_s) against reciprocal temperature will not be exactly linear, so that the values of E_{ss} and E_s in table II. 6 are means, corresponding most closely with the differential value as given by equation (II. 14) at the median temperature. There are two limiting cases: (i) $D_1 \gg D_2$, so that $E_{ss} \to E_1$,

and (ii) $D_1 \ll D_2$, so that $E_{ss} \to -\Delta H$; while in general $E_1 \leqslant E_{ss} \leqslant -\Delta H$. Theoretical treatments of surface diffusion refer to D_1.

II. 3.6. *Concentration dependence of* D_{ss}

Outside the Henry law range of adsorption the curvature of the isotherms implies that D_{ss} (and D_s) will depend upon the concentration of adsorbed molecules (Ash *et al.* 1967). In this region the relation $K_s = D_{ss} A k_s$ (equation II. 7) must for our boundary conditions be replaced by

$$K_s = \frac{\epsilon}{C_{0g}} \int_0^{C_{0g}} D_{ss} A \left(\frac{dC'_s}{dC_g} \right) dC_g, \qquad \text{(II. 16)}$$

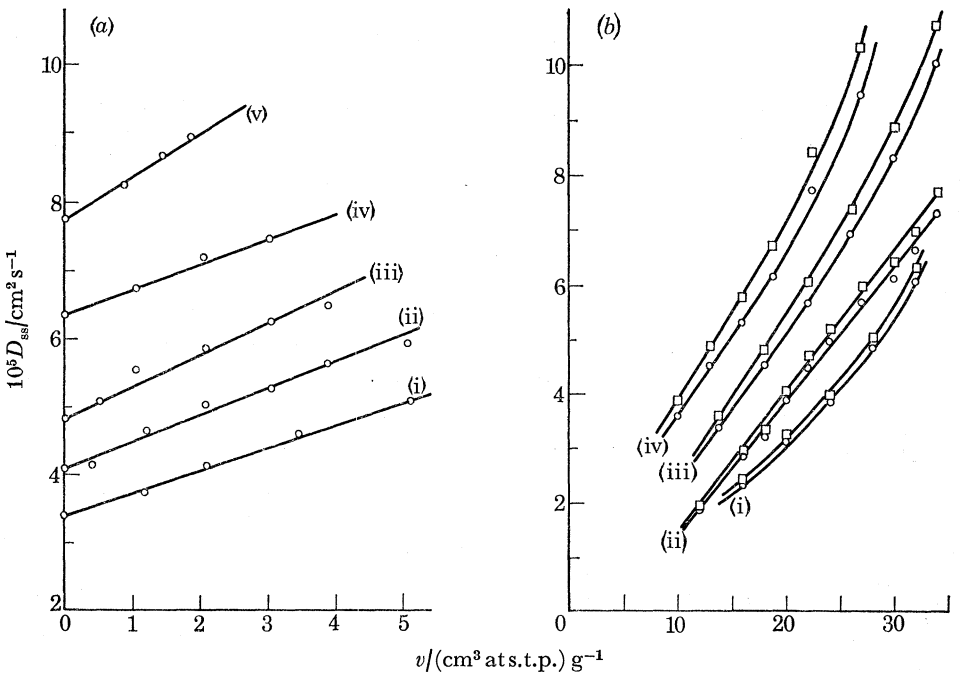

FIGURE II. 6. Concentration dependence of steady-state surface diffusion coefficients. (*a*) Kr in membrane L: (i) 308.15 K; (ii) 320.65 K; (iii) 333.15 K; (iv) 352.90 K; (v) 378.00 K. (*b*) C_3H_8 in membrane M: ○, minimum values; □, maximum values. (i) 320.65 K; (ii) 352.90 K; (iii) 333.15 K; (iv) 378.00 K.

where C_{0g} is the gas phase concentration per cm^3 of porous medium at $x = 0$ and C_g at $x = l$ tends to zero. So long as there is no blockage of gas phase transport by the adsorbed film it is necessary that the product $D_{ss}(dC'_s/dC_g)_T$ and K_s remain independent of C'_s (Ash *et al.* 1967). Figures II. 6*a* and *b* show concentration dependencies of D_{ss} for Kr in Carbolac L and C_3H_8 in Carbolac M. Both gases gave curved isotherms in this sorbent (part I), but only with C_3H_8 was the adsorption sufficient to block partially the gas phase flow and so to make $K = K_s + K_g$ depend upon pressure (figure II. 2). Using helium as an external indicator gas to measure K_g ($K_g = K_g^{He}\sqrt{(M_{He}/M)}$) gives therefore for propane an overestimate of K_g and so an underestimate of K_s ($K_s = K - K_g$). On the other hand, the assumption that $K_g = 0$ for propane leads to an overestimate of K_s. D_{ss} was accordingly calculated from K_s in equation (II. 16) using both assumptions so as to give lower and upper limits (figure II. 6*b*). Values of D_{ss} for the limits are close together and the very strong concentration dependence of D_{ss} is manifest.

II. 3.7. *Time-lags and blind pore character*

In a porous medium part of the transport during transient flow may be into blind pores. This part of the total flow decays to zero when the steady state is reached. Since the geometry of blind pores may differ from that of through channels, the instantaneous values of D_s and D_g at any cross-section could be time-dependent. Thus D_s and D_g, measured for the whole medium by the time-lag method (equations (II. 10) and (II. 11)), would be time averages over a period at least equal to the time-lag and also averages throughout the length of the medium (Barrer & Gabor 1960). This view was developed quantitatively by Ash *et al.* (1968), when it was noted that differences existed between the measured time-lag L and that quantity, L_1, defined by

$$lJ_\infty(C_0)\, L_1 = \int_0^l xC(x)\, \mathrm{d}x. \tag{II. 17}$$

Here $J_\infty(C_0)$ is the (concentration dependent) value of the total molecular flux through unit cross-section when C_0 is the value of $C(x)$ at $x = 0$ and $C(x)$ is the total concentration in molecules per cm^3 of porous medium bounded by planes $x = 0$ and $x = l$. The difference $(L_1 - L)$ defines a quantity Δ:

$$\Delta = L_1 - L, \tag{II. 18}$$

which may be influenced either by pore structures progressively changing with x, which make the local values of D_s and D_g at any plane x-dependent, or by the transient fluxes associated with blind-pore character which makes them time-dependent. The x-dependence can, however, be minimized or eliminated by making the membrane in increments, and where membranes are made by compaction x-dependence influences Δ in the opposite way to blind pores (Ash *et al.* 1968). Positive values of Δ result from the role of blind pores and it was shown that

$$2J_\infty(C_0)\, \Delta = Q_B(0), \tag{II. 19}$$

where $Q_B(0)$ is the quantity of gas that has flowed in the x-direction through unit area of the ingoing face ($x = 0$) between $t = 0$ and ∞, and that is associated with the blind pore component of flow only. If adsorption follows the Henry law

$$Q_B(0) = (\epsilon_b + A_b k_s)\, C'_{0g} l, \tag{II. 20}$$

where ϵ_b is a porosity associated with blind pore character and A_b is the corresponding area. C'_{0g} is the value of C'_g at $x = 0$. Since $K = J_\infty(C_0)\, l/C'_{0g}$ equations (II. 19) and (II. 20) may be combined to give

$$K\Delta = \tfrac{1}{2} l^2(\epsilon_b + A_b k_s). \tag{II. 21}$$

In a system where the Henry law is valid and under conditions for which equation (II. 17) is derived one has $C(x) = C_0(1 - x/l)$ and equation (II. 17) yields on integration

$$L_1 = l^2(\epsilon + Ak_s)/6K. \tag{II. 22}$$

Equations (II. 18), (II. 21) and (II. 22) then combine to give

$$KL = \tfrac{1}{6} l^2[(\epsilon - 3\epsilon_b) + k_s(A - 3A_b)]. \tag{II. 23}$$

In terms of A_g, the area per gram of carbon, one has $A_g = A/\rho(1 - \epsilon)$ where ρ is the density of the carbon and A as before is the area per cm^3 of membrane. Thus, for a series of gases each adsorbed according to the Henry law, a graph of KL against $A_g k_s$ should give a straight line of

slope $\frac{1}{6}l^2[\rho(1-\epsilon)-3A_b/A_g]$ and intercept $\frac{1}{6}l^2(\epsilon-3\epsilon_b)$. These lines are shown in figure II. 7 *a*, *b* and *c* for Carbolac L, Carbolac M and Graphon N respectively. From these graphs the blind pore parameters of table II. 7 were obtained. From the ratios ϵ_b/ϵ, ϵ_b is seen to be a significant fraction of ϵ, but A_b is a rather small fraction of A. However, ϵ_b and A_b may not represent the total blind porosity and area, especially since residual influence of x-dependence upon Δ could reduce its value.

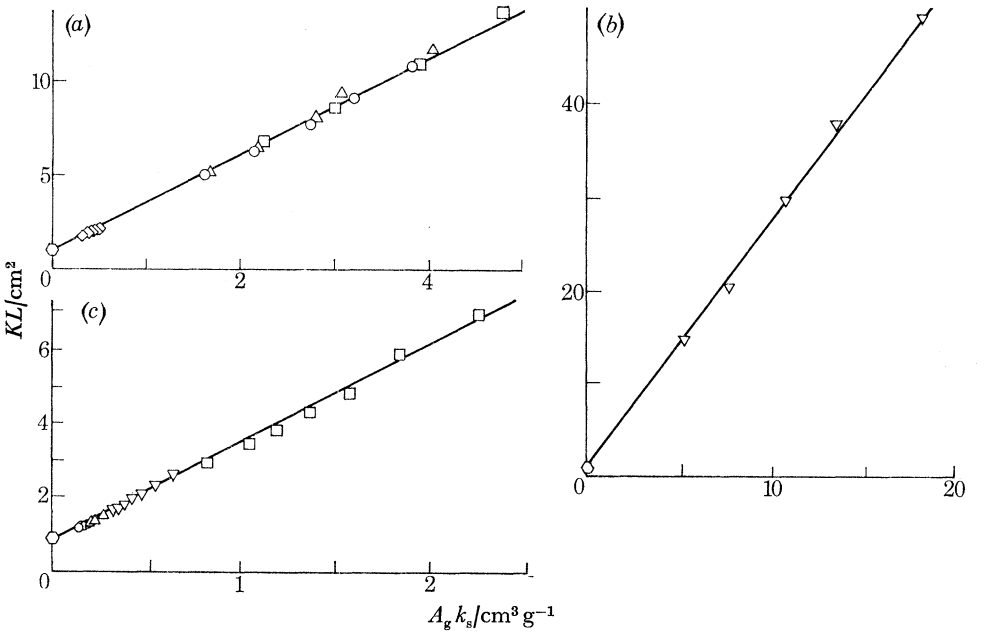

FIGURE II. 7. KL as a function of $A_g k_s$ for various gases. (*a*) Membrane L: ⬡, He; ◇, D_2; ○, Ar; △, N_2; □, CO. (*b*) Membrane M: ⬡, He; ▽, Kr. (*c*) Membrane N: ⬡, He; ○, Ar; ▽, Kr; □, Xe; △, N_2.

TABLE II. 7. PARAMETERS ASSOCIATED WITH BLIND-PORE CHARACTER

	membrane		
	L	M	N
ϵ_b/cm³ cm⁻³	0.053_8	0.035_2	0.042_6
A_b/m² cm⁻³	44.9	61.4	6.66
(ϵ_b/A_b)/nm	1.20	0.573	6.40
ϵ_b/ϵ	0.111	0.074_6	0.101
A_b/A	0.044	0.058	0.074

It is of interest that, once sufficient data are available for several gases in a given membrane to establish a linear graph of KL against $A_g k_s$ (or Ak_s), it should be possible if K and L are measured for further gases, to interpolate k_s for them. Thus an equilibrium property, k_s, could be estimated from kinetic ones. Adsorption must for these gases be in the Henry law range.

III. Thermo-osmosis of sorbable gases

III. 1. *Introduction*

Most non-isothermal flow measurements in porous media have involved gases where mobile adsorbed films do not contribute significantly to the transport (Hanley 1965, 1966; Hopfinger & Altman 1969; Rastogi, Singh & Singh 1969). An exception is the work of Gilliland *et al.* (1962), who assumed the driving force in surface flow to be the gradient in surface pressure. Hill (1956) considered the theory of non-isothermal flow of adsorbed molecules on the wall of a single capillary, but assumed that even for dilute films the mean free paths of migrating molecules were terminated by molecule–molecule collisions rather than by the far more numerous vibrational collisions with atoms of the sorbent. Accordingly, contrary to experiment (see, for example Barrer 1967) his surface diffusion coefficients were concentration dependent in the Henry law range. More recently irreversible thermodynamic aspects of simultaneous thermo-osmosis of adsorbed and gaseous molecules have been considered (Lassettre & Brooks 1961; Ash & Barrer 1963), and a stochastic treatment of non-isothermal surface flow on an ideal surface has also been developed (Wright 1971).

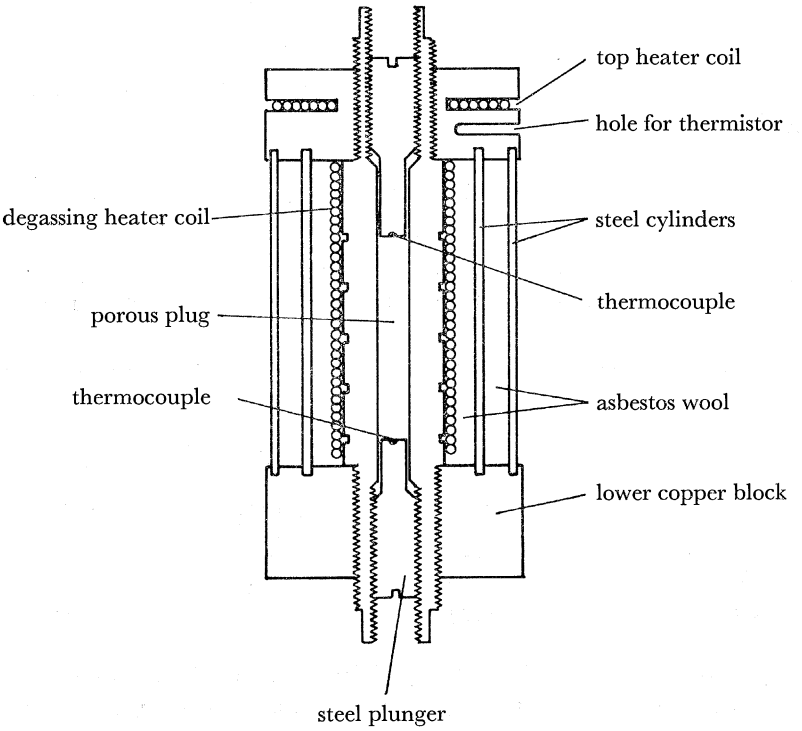

Figure III. 1. The membrane assembly.

In view of the large extra flows which can arise under isothermal conditions for sorbable gases in microporous membranes (part II) thermo-osmosis in the presence of these extra flows is of particular interest. Under isothermal conditions microporous membranes can be remarkably selective in separating strongly from weakly adsorbed gases (Ash *et al.* 1963*b*) so that thermo-osmosis of such gas pairs might also prove to be an interesting method of separation. Aspects of thermo-osmosis have accordingly been investigated using the membranes and sorbates already characterized under equilibrium and isothermal flow conditions.

III. 2. *Experimental*

The membrane assembly is shown in figure III. 1. The carbon membranes, which were about 4 cm long, were contained in stainless-steel plug holders, and further confined by light contact with two stainless-steel plungers. The junction of a copper-constantan thermocouple was fixed into a groove in the flat face of each plunger with a high-temperature epoxy resin and the surface ground flat. These thermocouples were then used to measure the temperatures T_0 and T_l at the faces $x = 0$ and $x = l$ of the membrane. Each insulated thermocouple lead passed along a groove in the side of the plunger and was taken out through pinch seals filled with epoxy resin. In addition five copper-constantan thermocouples were fixed with the resin into grooves turned, at approximately 1 cm intervals, on the outside of the plug holder. Over them was wound a layer of asbestos paper and then a coil of asbestos-covered wire which was used as a heating coil for degassing the membrane.

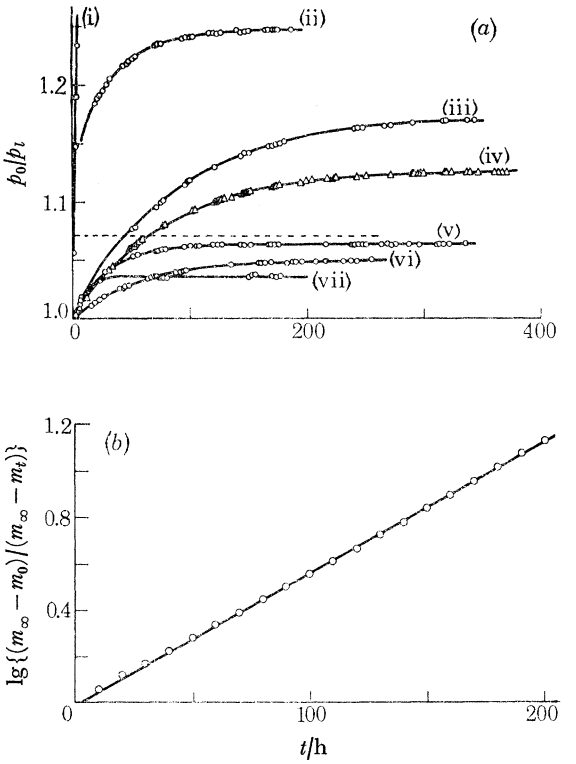

FIGURE III. 2. (*a*) Typical transient approach curves. $T_l = 308.15$ K. (i) C_3H_8 (in M): $T_0 = 378.0$ K; (ii) CO_2 (in L): $T_0 = 352.9$ K; (iii) Kr (in L): $T_0 = 378.0$ K; (iv) Kr (in M): $T_0 = 352.9$ K; (v) H_2 (in L): $T_0 = 352.9$ K; (vi) He (in M): $T_0 = 352.9$ K; (vii) Kr (in N): $T_0 = 363.15$ K. Dashed curve denotes $(T_0/T_l)^{\frac{1}{2}} = (352.9/308.15)^{\frac{1}{2}}$. (*b*) $\lg(m_\infty - m_0)/(m_\infty - m_t)$ as a function of time: Kr (in M): $T_l = 308.15$ K, $T_0 = 352.9$ K.

Copper blocks fitted to the ends of the plug holder were screwed up to hold two stainless-steel cylindrical tubes coaxial with the carbon plug. Asbestos wool was packed between the plug holder and the two cylinders, to provide heat insulation and help ensure a linear temperature gradient along the plug holder. The upper copper block was provided with a deep cavity to take heating coil windings, and a hole for the temperature control thermistor. The whole unit was joined to the rest of the apparatus by Kovar graded metal-glass seals, silver soldered to the stainless-steel membrane holder.

Experiments were carried out as follows. The top copper block was heated electrically and the lower block immersed in a thermostat. When the desired temperature gradient was established across the membrane, with the lower face of the plug at 35 °C for all runs, gas was admitted to the plug with the two sides interconnected. When the pressure ceased to fall (the fall being due to establishment of sorption equilibrium in the membrane) the tap connecting the two sides was closed, and the subsequent change in the ratio of pressures in the volumes attached to hot and cold sides of the membrane was plotted against time (figure III. 2*a*).

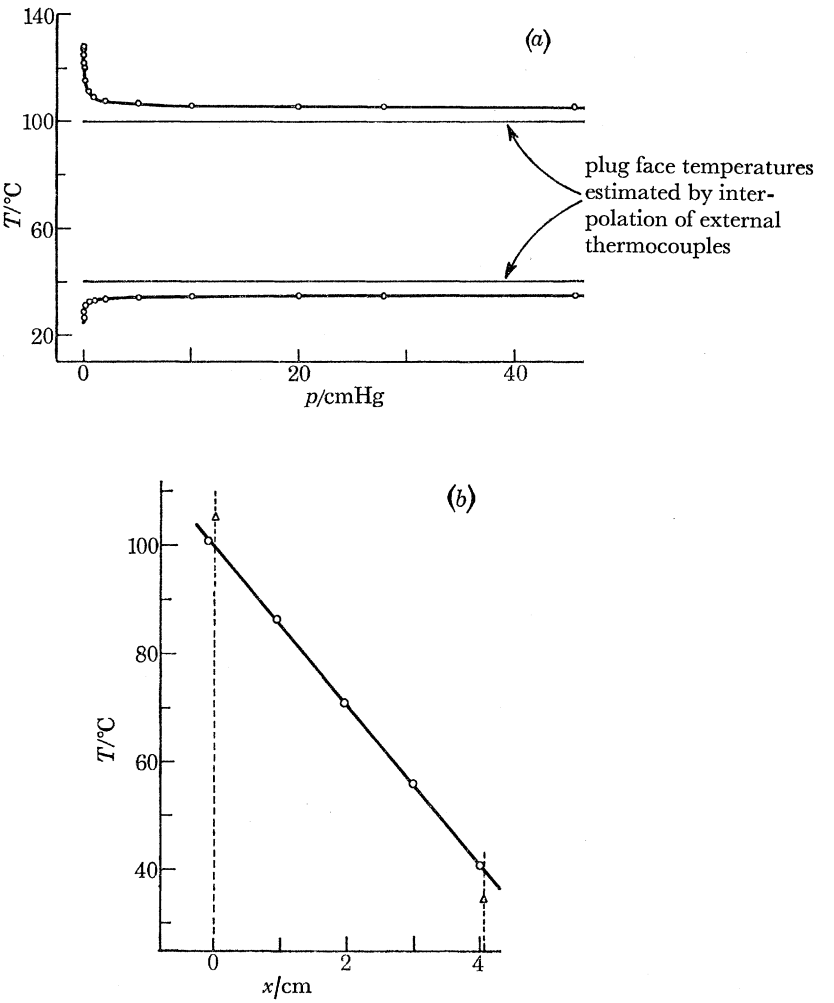

FIGURE III. 3. (*a*) Effect of gas pressure on temperature readings of plunger thermocouples. (*b*) Comparison of temperatures recorded with thermocouples: ○, outer thermocouples; △, plunger thermocouples; – – –, position of membrane faces.

With helium as the flowing gas the temperatures of the two thermocouples at the hot and cold faces of the plug were found at low pressures to depend upon the pressure in the way shown in figure III. 3*a*. Similar curves were observed with neon and accordingly all runs were made at pressures in excess of 15 cmHg. Above this pressure figure III. 3*b* compares the temperature readings of the outer thermocouples with those of the two thermocouples at the 'hot' and 'cold' faces of the plug. The outer thermocouples establish that there is a linear gradient, but that there

is a temperature difference between each face of the plug and the temperature at the corresponding height on the outer surface of the plug holder. Thus at $x = 0$ and $x = l$ there is a radial temperature gradient of about 5 °C between the axis of the cell and the outer surface of the plug holder. The radial gradients across the carbon faces must be less than this. The axial thermocouples at $x = 0$ and $x = l$ were, as noted earlier, used to give T_0 and T_l.

In close correspondence with the results of Crowe (1957) the rate at which the thermo-osmotic steady state was established agreed for larger t with the relation

$$\frac{m_\infty - m_t}{m_\infty - m_0} = \exp(-kt), \tag{III. 1}$$

where

$$m = (p_0/p_l - 1). \tag{III. 1a}$$

In these relations p_0 and p_l are the pressures at the two faces $x = 0$ and $x = l$ of the carbon plugs, k is a constant and the subscripts to m indicate the times to which the m refer. Because the final pressure ratio p_0/p_l was established only slowly (figure III. 2*a*) and because over the early stage the kinetics did not follow equation (III. 1) exactly, a modification of Guggenheim's (1926) method of obtaining m_∞ was used, in which values of m were measured from time $t = z$ rather, than from $t = 0$. Then at $t = t_j$

$$m_j = (m_\infty - m_z)(1 - \exp(-kt_j)). \tag{III. 2}$$

Figure III. 2*b* shows a typical plot of $\lg[(m_\infty - m_0)/(m_\infty - m_t)]$ against t, employing a value of m_∞ derived using the modified Guggenheim procedure.

III. 3. *Theoretical aspects*

Because the formulation of non-isothermal flow is best made in terms of irreversible thermodynamics the relations between the phenomenological coefficients of this treatment and the usual permeabilities and diffusion coefficients must be found. Further, in considering the extra flow, J_s, due to mobile adsorbed films in a concentration gradient, there is a choice in the way in which the pore space is divided and in the subdivision of the molecules in this space.

Thus, of the total pore volume, ϵ, in $cm^3\,cm^{-3}$ one may (cf. part I) consider that $A\delta$ is associated with the adsorbed state of the gas while $(\epsilon - A\delta)$ comprises the gas phase. The absolute sorption, C^s, is then the total number of molecules in $A\delta$ while C^g is the number in $(\epsilon - A\delta)$. Since $A\delta$ and $(\epsilon - A\delta)$ refer to a cm^3 of porous medium, C^s and C^g are also numbers of molecules per cm^3 of the porous medium. Alternatively, with no division of ϵ in the above way, one may consider the Gibbs excess, C_s in molecules per cm^3 of medium and the total number, C_g, of molecules which would be present per cm^3 of the medium in absence of adsorption. If C is the total number of molecules per cm^3 of medium then

$$C = C^s + C^g = C_s + C_g = AC'_s + \epsilon C'_g. \tag{III. 3}$$

Also

$$C^s = A(C'_s + \delta C'_g); \quad C^g = (\epsilon - A\delta)\, C'_g. \tag{III. 4}$$

As before, C'_s is the Gibbs excess per unit area and C'_g the number of molecules per cm^3 of gas phase in equilibrium with C'_s.

III. 3.1. *Isothermal flow*

As in part II, the total flow, J, per unit cross-section normal to x will be considered as the sum of $J_s + J_g$, respectively the extra flow and the flow which would be expected in absence of

adsorption. The steady state flow in molecules per second per unit cross-section can formally be expressed in several equivalent ways:

$$\left.\begin{aligned} J &= K\frac{\Delta C'_g}{l} = K_s\frac{\Delta C'_g}{l} + K_g\frac{\Delta C'_g}{l}, \\ J &= -D\frac{dC}{dx} = -D_{ss}\frac{dC_s}{dx} - D_{gs}\frac{dC_g}{dx}, \\ J &= -Cl_{11}\frac{d\mu}{dx} = -C_s l^s_{11}\frac{d\mu}{dx} - C_g l^g_{11}\frac{d\mu}{dx} = -C^s\lambda^s_{11}\frac{d\mu}{dx} - C^g\lambda^g_{11}\frac{d\mu}{dx}, \end{aligned}\right\} \quad \text{(III. 5)}$$

where μ is the chemical potential, the l and λ are mobility coefficients and $\Delta C'_g = (C'_g)_{x=0} - (C'_g)_{x=l}$. From these relations one obtains

$$\left.\begin{aligned} K &= K_s + K_g, \\ D(A\sigma + \epsilon) &= D_{ss}A\sigma + \epsilon D_{gs}, \\ Cl_{11} &= C_s l^s_{11} + C_g l^g_{11} = C^s\lambda^s_{11} + C^g\lambda^g_{11}, \end{aligned}\right\} \quad \text{(III. 6)}$$

where $\sigma = dC'_s/dC'_g$ is the slope of the isotherm which in the Henry law range is the Henry law constant k_s. Term-by-term comparison of the last of the relations (III. 5) gives

$$C_s l^s_{11} = C^s\lambda^s_{11}, \quad C_g l^g_{11} = C^g\lambda^g_{11}. \quad \text{(III. 7)}$$

The relations between the K's and D's are found by integrating the second of the equations (III. 5) with respect to x between 0 and l and comparing the result with the first of these equations:

$$\left.\begin{aligned} \frac{Jl}{\Delta C} = K\frac{\Delta C'_g}{\Delta C} = \frac{K\Delta C_g}{\epsilon\Delta C} &= \frac{1}{\Delta C}\int_{C_l}^{C_0} D(C)\,dC = \tilde{D}(C), \\ \frac{K_s}{\epsilon}\frac{\Delta C_g}{\Delta C_s} &= \tilde{D}_{ss}(C_s), \\ \frac{K_g}{\epsilon} &= \tilde{D}_{gs}(C_g). \end{aligned}\right\} \quad \text{(III. 8)}$$

The $\tilde{D}$ are integral diffusion coefficients over the concentration intervals ΔC between $x = 0$ and $x = l$. In the Henry law range where the ratios $\Delta C_g/\Delta C$ and $\Delta C_g/\Delta C_s$ are both constants, and for K, K_s and K_g independent of C_g, it follows that D, D_{ss} and D_{gs} are constants, so that equations (III. 8) become

$$\left.\begin{aligned} K &= (Ak_s + \epsilon)\,D = Ak_s D_{ss} + \epsilon D_{gs}, \\ K_s &= Ak_s D_{ss}, \\ K_g &= \epsilon D_{gs}. \end{aligned}\right\} \quad \text{(III. 9)}$$

The relations between the K and the l_{11} may be found by integration of the third of the relations (III. 5) w.r.t. x between $x = 0$ and $x = l$ and comparing the result with the first of the equations (III. 5). With $d\mu = RT\,d\ln a = RT\,d\ln C_g$ (where a denotes activity) one obtains

$$\left.\begin{aligned} K &= \frac{\epsilon RT}{\Delta C_g}\int_{C_{gl}}^{C_{g0}}\frac{Cl_{11}}{C_g}\,dC_g, \\ K_s &= \frac{\epsilon RT}{\Delta C_g}\int_{C_{gl}}^{C_{g0}}\frac{C_s l^s_{11}}{C_g}\,dC_g, \\ K_g &= \frac{\epsilon RT}{\Delta C_g}\int_{C_{gl}}^{C_{g0}} l^g_{11}\,dC_g. \end{aligned}\right\} \quad \text{(III. 10)}$$

If K, K_s and K_g are each constant over the interval $\Delta C_g = C_{g0} - C_{gl}$ between $x = 0$ and $x = l$ then Cl_{11}/C_g, $C_s l^s_{11}/C_g$ and l^g_{11} must also be constants and equations (III. 10) become

$$\left.\begin{aligned} K &= \frac{\epsilon RT}{C_g} Cl_{11} = \frac{\epsilon RT}{C_g}(C_s l^s_{11} + C_g l^g_{11}) = \frac{\epsilon RT}{C_g}(C^s\lambda^s_{11} + C^g\lambda^g_{11}), \\ K_s &= \frac{\epsilon RT}{C_g} C_s l^s_{11} = \frac{\epsilon RT}{C_g} C^s\lambda^s_{11}, \\ K_g &= \epsilon RT l^g_{11} = \frac{\epsilon RT}{C_g} C^g\lambda^g_{11}. \end{aligned}\right\} \qquad \text{(III. 11)}$$

In absence of a viscous flow component in the gas phase, as in the present work, the K are often independent of C_g well outside the Henry law range (cf. part II).

Next one obtains directly from comparison of the last two of the equations (III. 5) the relations between the D and the l_{11}:

$$\left.\begin{aligned} D &= RTl_{11}\frac{\mathrm{d}\ln C_g}{\mathrm{d}\ln C}, \\ D_{ss} &= RTl^s_{11}\frac{\mathrm{d}\ln C_g}{\mathrm{d}\ln C_s} = RT\frac{C^s\lambda^s_{11}}{C_s}\frac{\mathrm{d}\ln C_g}{\mathrm{d}\ln C_s}, \\ D_{gs} &= RTl^g_{11} = RT\frac{C^g\lambda^g_{11}}{C_g}. \end{aligned}\right\} \qquad \text{(III. 12)}$$

Finally from comparison of the first and the last of the equations (III. 5) and (III. 11) one obtains:

$$\left.\begin{aligned} K_s/K &= \frac{C_s l^s_{11}}{C_s l^s_{11} + C_g l^g_{11}} = \frac{C^s\lambda^s_{11}}{C^s\lambda^s_{11} + C^g\lambda^g_{11}}, \\ K_g/K &= \frac{C_g l^g_{11}}{C_s l^s_{11} + C_g l^g_{11}} = \frac{C^g\lambda^g_{11}}{C^s\lambda^s_{11} + C^g\lambda^g_{11}}. \end{aligned}\right\} \qquad \text{(III. 13)}$$

Equations (III. 6) to (III. 13) give all the general and special relations between the several coefficients needed in part III.

For a non-sorbed gas C'_s, C_s and k_s are zero and the division of ϵ into $A\delta$ and $(\epsilon - A\delta)$ no longer has any significance. Accordingly

$$K = K_g = \epsilon D = \epsilon D_{gs} = \epsilon RTl^g_{11}. \qquad \text{(III. 14)}$$

This situation is approximated by helium. For any sorbed gas it is assumed, as in part II, that at constant temperature

$$D_{gs} = D^{He}_{gs}\sqrt{(M_{He}/M)}; \quad K_g = K^{He}_g\sqrt{(M_{He}/M)}, \qquad \text{(III. 15)}$$

in which case one has

$$\left.\begin{aligned} l^g_{11} &= (l^g_{11})_{He}\sqrt{(M_{He}/M)}, \\ \lambda^g_{11} &= (l^g_{11})_{He}[\epsilon/(\epsilon - A\delta)]\sqrt{(M_{He}/M)}. \end{aligned}\right\} \qquad \text{(III. 16)}$$

Knowing l^g_{11} or λ^g_{11} the first of the equations (III. 11) then serves to obtain l^s_{11} or λ^s_{11}, when K is independent of C_g.

III. 3.2. *Non-isothermal flow*

When flow occurs across the membrane under the combined influence of gradients in concentration and temperature the flux per unit cross-section in terms of C_s and C_g is† (Ash & Barrer 1963)

$$J = J_s + J_g = -C_s\left\{l^s_{11}\,T\frac{\partial(\mu/T)}{\partial x} + \frac{l^s_{12}}{T}\frac{\partial T}{\partial x}\right\} - C_g\left\{l^g_{11}\,T\frac{\partial(\mu/T)}{\partial x} + \frac{l^g_{12}}{T}\frac{\partial T}{\partial x}\right\}, \qquad \text{(III. 17)}$$

where $C_s l^s_{12}$ and $C_g l^g_{12}$ are cross-coefficients for heat and matter flows for J_s and J_g respectively. If T_l, the temperature at $x = l$, is kept constant and T_0 at $x = 0$ is allowed to vary then, in the thermo-osmotic steady state for which $J = 0$, Ash & Barrer (1963) showed that the heat of transport Q_0 at T_0 is given by

$$Q_0 = RT_0^2\,\partial/\partial T_0[\ln(p_l/p_0)]_{T_l} = \left[\frac{C_s l^s_{12} + C_g l^g_{12}}{C_s l^s_{11} + C_g l^g_{11}} - H_g^{\ominus}\right]_{x=0}. \qquad \text{(III.18)}$$

In this relation $H_g^{\ominus}$ is the standard enthalpy of the gas at T_0 and p_l, p_0 are the pressures at $x = l$ and $x = 0$ when $J = 0$.

Equation (III. 18) can be re-arranged to

$$Q_0 = \left[\frac{l^s_{12}}{l^s_{11}} - H_g^{\ominus}\right]\frac{C_s l^s_{11}}{C_s l^s_{11} + C_g l^g_{11}} + \left[\frac{l^g_{12}}{l^g_{11}} - H_g^{\ominus}\right]\frac{C_g l^g_{11}}{C_s l^s_{11} + C_g l^g_{11}}. \qquad \text{(III. 19)}$$

From equation (III. 13) and with

$$Q_g = l^g_{12}/l^g_{11} - H_g^{\ominus}, \qquad \text{(III. 20)}$$

$$Q_s = l^s_{12}/l^s_{11} - H_g^{\ominus}, \qquad \text{(III. 21)}$$

equation (III. 19) becomes

$$Q_0 = Q_s K_s/K + Q_g K_g/K, \qquad \text{(III. 22)}$$

wherein Q_s is the heat of transport per mol for the molecules comprising J_s (which is partly on the surface and partly in the gas phase (Barrer & Gabor 1960)); and Q_g is this heat for J_g. Increasing the temperature causes K_s/K to decrease and K_g/K to grow, so that at high enough temperature $Q_0 \to Q_g$. Conversely, at low enough temperatures, with $K_s \gg K_g$, $Q_0 \to Q_s$.

The amounts of heat transported per mol in isothermal flow in J_s and J_g are respectively Q_s^* and Q_g^* where (Denbigh 1951)

$$Q_s^* = l^s_{12}/l^s_{11} = \lambda^s_{12}/\lambda^s_{11}, \quad Q_g^* = l^g_{12}/l^g_{11} = \lambda^g_{12}/\lambda^g_{11}. \qquad \text{(III. 23)}$$

Accordingly, equation (III. 22) can be rewritten as

$$Q_0 + H_g^{\ominus} = Q_s^* K_s/K + Q_g^* K_g/K. \qquad \text{(III. 24)}$$

III. 4. *Results and discussion*

Heats of transport, phenomenological coefficients and isobaric permeabilities are considered in the following sections.

III. 4.1. *Heats of transport*

For constant T_l, $\lg(p_0/p_l)$ was plotted against K/T_0 for each of a series of gases in the three membranes (figures III. 4*a* to *d*). At each value of T_0 the corresponding heat of transport, Q_0, is

$$Q_0 = 2.303R\frac{\partial}{\partial(1/T_0)}[\lg(p_0/p_l)]_{T_l}. \qquad \text{(III. 25)}$$

† Ash & Barrer considered fluxes J'_s and J'_g solely in the surface and in the gas phases rather than the extra flux J_s and the flux J_g which could occur in absence of adsorption. The formal treatment remains the same, although the coefficients l or λ would differ numerically.

Plots of $-Q_0$ against T_0 are presented in figure III. 5*a*, *b* and *c* for each membrane. The method used for determining Q_0 is independent of T_l, provided only that T_l is kept constant.

The heats of transport showed the following consistent pattern. Q_0 was negative in all cases. For strongly adsorbed gases $-Q_0$ decreased as T_0 increased, in accord with equation (III. 24). For less and less strongly adsorbed gases the negative slope of the curve of $-Q_0$ against T_0 decreased until for Ne, H_2, D_2 and He the slope changed sign and became positive. The dashed

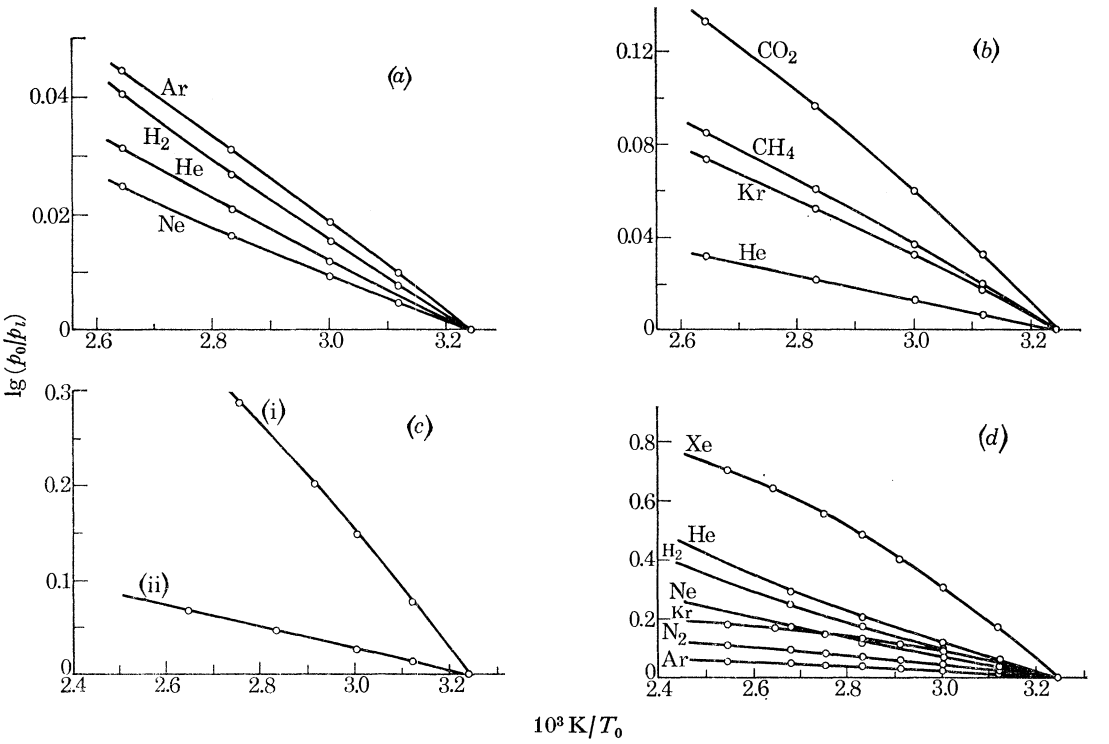

FIGURE III. 4. Lg (p_0/p_l) for a series of gases as a function of reciprocal temperature, K/T_0 (T_l/K = constant). (*a*) Membrane L; (*b*) membrane M; (*c*) (i) C_3H_8 in M, (ii) Kr in L; (*d*) membrane N.

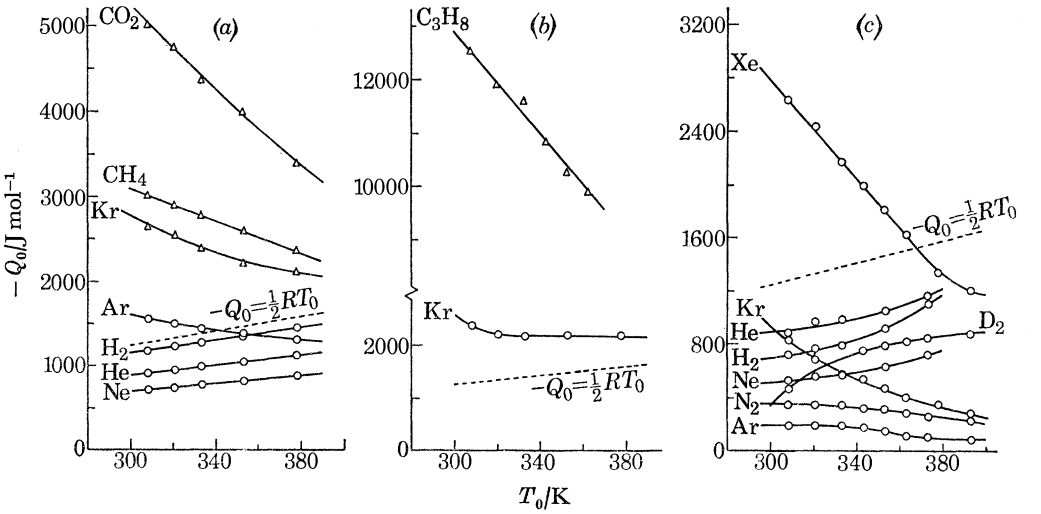

FIGURE III. 5. Overall heats of transport as functions of temperature. (*a*), (*b*): ○, membrane L; △, membrane M; (*c*) membrane N.

lines in figure III. 5 give $-Q_0 = \frac{1}{2}RT_0$ which is the ideal value expected for a gas transported by molecular streaming (Knudsen flow). None of the gases behaved exactly in this way. However for He, H_2 and Ne in the Carbolac membranes $-Q_0$ was almost proportional to T_0, so that for these systems

$$Q_0 = \beta(-\tfrac{1}{2}RT_0), \tag{III. 26}$$

where β is a constant. Some values of β are given for Carbolac membranes L and M in table III. 1. In the Graphon membrane the plots of $-Q_0$ against T_0 for He, H_2, D_2 and Ne were not fully linear (figure III. 5*c*). Accordingly values of β were determined from equation (III. 26) at $T_0 = 353.15$ K, and are also given in the table. The values of β are often well below unity and tend to be smaller the heavier the diffusing gas.

The molecules listed in table III. 1 are the most weakly adsorbed. With $H_g^{\ominus} = \frac{5}{2}RT_0$ for monatomic and $\frac{7}{2}RT_0$ for diatomic gases, Q_{id}^* for an ideal Knudsen gas is $2RT_0$ for monatomic and $3RT_0$ for diatomic gases. By adding $H_g^{\ominus}$ to the experimental values of Q_0 for He, H_2, D_2 and Ne one obtains $Q_0^* \sim Q_g^*$ for these gases. The ratios Q_g^*/Q_{id}^* are rather near unity (table III. 1).

TABLE III. 1. β AND Q_g^*/Q_{id}^* FOR CARBOLAC AND GRAPHON MEMBRANES

gas	membrane	β†	Q_g^*/Q_{id}^*
Knudsen gas	—	1.00	1.00
H_2	L	0.92	1.01
H_2	N	0.63	1.06
D_2	N	0.54	1.08
He	L	0.71	1.07
He	M	0.72	1.07
He	N	0.72	1.07
Ne	L	0.56	1.11
Ne	N	0.43	1.14

† β and Q_g^*/Q_{id}^* for the Graphon membrane (N) refer only to $T_0 = 353.15$ K.

For more strongly adsorbed gases (N_2, Ar, Kr and Xe) Q_0 is significantly influenced by the larger values of J_s. One may now estimate Q_s^* and $Q_s = Q_s^* - H_g^{\ominus}$, using equation (III. 24), for the two limiting cases:

(i) $Q_g = -\frac{1}{2}RT_0$ (and so $\beta = 1$, $Q_g^* = Q_{id}^*$);

and (ii) $Q_g = 0$ ($\beta = 0$, $Q_g^* = H_g^{\ominus}$).

The results of these calculations are given in tables III. 2 and III. 3. Negative values of Q_s were always found for $Q_g = 0$, but for $Q_g = -\frac{1}{2}RT_0$ positive values were sometimes observed in Graphon N. Since positive values are not possible, as shown in the next section, such values are not recorded in table III. 3. Q_s is very sensitive to the value taken for Q_g. The low values of $-Q_0$ at the highest temperatures, especially for Graphon N (e.g. $-Q_0 = 92.5$ J mol^{-1} for Ar in N at 393.15 K) certainly indicate very small values of Q_g and that β approaches zero.

The origin of small values of β is of considerable interest, since as β approaches zero Q_g^* must approach $H_g^{\ominus}$. This happens in viscous flow, but in the present work the permeabilities K were independent of pressure (part II) so that viscous flow was absent. It is important to know whether the radial gradient in temperature at the ingoing face (§ III. 2) could significantly influence Q_g^* and hence Q_g.

It is assumed that transport of a non-sorbed gas within the membrane accords with ideal

Knudsen conditions for which $Q_g = -\frac{1}{2}RT$. It is probable that pressures just within the membrane surfaces at $x = 0$ and $x = l$ equal pressures just outside, and that rapid flow in the gas phase maintains these pressures substantially constant over these surfaces. This condition requires in presence of the radial temperature gradients that $p(x,r)/T^{\frac{1}{2}}(x,r)$ is not constant throughout the medium, as would be the case for a Knudsen gas in the steady state if the temperature T depended only upon x. The non-constancy of $p/\sqrt{T}$ means in turn that circulation will occur continually, within the membrane, and also within that part of the membrane and the gas phase adjacent to the surfaces at $x = 0$ and $x = l$.

TABLE III. 2. Q_s^* AND Q_s/kJ mol^{-1} FOR CARBOLAC MEMBRANES†

(*a*) membrane L

system ...	Ar				Kr			
	$Q_g = -\frac{1}{2}RT_0$		$Q_g = 0$		$Q_g = -\frac{1}{2}RT_0$		$Q_g = 0$	
T_0/K	Q_s^*	$-Q_s$	Q_s^*	$-Q_s$	Q_s^*	$-Q_s$	Q_s^*	$-Q_s$
308.15	4.6_8	1.7_2	3.9_1	2.5_0	3.7_0	2.7_1	3.3_1	3.1_0
320.65	5.0_7	1.5_9	4.2_0	2.4_7	4.1_7	2.5_0	3.7_2	2.9_4
333.15	5.4_5	1.4_8	4.4_6	2.4_7	4.4_6	2.4_7	3.9_5	2.9_8
352.90	6.0_2	1.3_2	4.8_5	2.4_9	4.8_7	2.4_7	4.2_4	3.0_9
378.00	6.7_8	1.0_8	5.3_9	2.4_7	5.4_0	2.4_6	4.6_0	3.2_6

(*b*) membrane M

system ...	Kr				CH_4				CO_2			
	$Q_g = -\frac{1}{2}RT_0$		$Q_g = 0$		$Q_g = -\frac{1}{2}RT_0$		$Q_g = 0$		$Q_g = -\frac{1}{2}RT_0$		$Q_g = 0$	
T_0/K	Q_s^*	$-Q_s$	Q_s^*	$-Q_s$	Q_s^*	$-Q_s$	Q_s^*	$-Q_s$	Q_s^*	$-Q_s$	Q_s^*	$-Q_s$
308.15	3.3_3	3.0_7	2.9_4	3.4_6	6.8_1	3.5_9	6.3_8	4.0_2	4.2_0	5.5_5	4.0_1	5.7_4
320.65	3.7_2	2.9_4	3.2_7	3.3_9	7.3_8	3.4_8	6.8_9	3.9_6	4.9_0	5.3_3	4.6_7	5.5_5
333.15	4.1_7	2.7_6	3.6_5	3.2_8	7.9_5	3.3_7	7.3_8	3.9_4	5.7_6	4.9_5	5.4_9	5.2_2
352.90	4.8_0	2.5_3	4.1_5	3.1_8	8.9_2	3.1_3	8.2_1	3.8_4	6.8_8	4.5_9	6.5_2	4.9_4
378.00	5.4_8	2.3_7	4.6_7	3.1_9	10.2_5	2.8_0	9.3_4	3.7_1	8.5_3	3.9_4	8.0_6	4.4_1

† Source of enthalpy data for H_2, N_2, CH_4 and CO_2: *National Bur. Stds, Wash. Circ.* No. 564, 1955, Table of thermal properties of gases.

This situation can be considered further. For the Knudsen gas the steady-state pressures ($J = 0$) at $x = 0$ and $x = l$ are p_0 and p_l. The flux J through unit area of the annulus $2\pi r\,dr$ at chosen radius r is

$$[J(x,r)]_r = -\frac{K_g^0}{R}\frac{\partial}{\partial x}\left[\frac{p(x,r)}{T^{\frac{1}{2}}(x,r)}\right]_r, \tag{III. 27}$$

where $K_g^0\sqrt{T} = K_g$, the isothermal permeability at T, and so K_g^0 is independent of T (or x). The steady-state condition for any cross-section is

$$0 = -2\pi\int_0^a r[J(x,r)]_r\,dr = 2\pi\frac{K_g^0}{R}\int_0^a r\frac{\partial}{\partial x}\left[\frac{p(x,r)}{T^{\frac{1}{2}}(x,r)}\right]_r dr \tag{III. 28}$$

where a is the radius of the cylindrical membrane. Then also

$$0 = \frac{K_g^0}{R}\int_0^l\int_0^a r\frac{\partial}{\partial x}\left[\frac{p(x,r)}{T^{\frac{1}{2}}(x,r)}\right]_r dr\,dx = \frac{K_g^0}{R}\int_0^a r\left[\frac{p_l}{T_l^{\frac{1}{2}}(r)} - \frac{p_0}{T_0^{\frac{1}{2}}(r)}\right]dr. \tag{III. 29}$$

The last expression on the right-hand side assumes that the order of integration may be changed.

PHILOSOPHICAL TRANSACTIONS OF THE ROYAL SOCIETY A MATHEMATICAL, PHYSICAL & ENGINEERING SCIENCES

TABLE III.3. Q_s^* AND Q_s/kJ mol^{-1} FOR GRAPHON MEMBRANE N

system ...	N_2			Ar			Kr			Xe			
	$Q_g = -\frac{1}{2}RT_0$	$Q_g = 0$		$Q_g = -\frac{1}{2}RT_0$	$Q_g = 0$		$Q_g = -\frac{1}{2}RT_0$	$Q_g = 0$		$Q_g = -\frac{1}{2}RT_0$		$Q_g = 0$	
T_0/K	Q_s^*	Q_s^*	$-Q_s$	Q_s^*	Q_s^*	$-Q_s$	Q_s^*	Q_s^*	$-Q_s$	Q_s^*	$-Q_s$	Q_s^*	$-Q_s$
308.15	10.4	7.9_3	1.03	7.9_8	5.90	0.50_2	5.91	4.91	1.49	3.30	3.11	2.86	3.55
320.65	11.0	8.2_7	1.06	8.4_8	6.14	0.52_7	6.54	5.41	1.26	3.80	2.87	3.28	3.38
333.15	11.7	8.5_8	1.11	8.9_8	6.37	0.55_1	7.1_2	5.83	1.10	4.40	2.52	3.79	3.13
343.15	12.3	8.9_2	1.06	9.4_0	6.60	0.52_8	7.4_7	6.05	1.08	4.86	2.27	4.18	2.95
353.15	12.9	9.1_9	1.09	9.9_6	6.9_0	0.44_5	7.9_4	6.37	0.96_8	5.35	1.99	4.59	2.75
363.15	13.5	9.5_3	1.04	10.5	7.1_9	0.36_2	8.4_1	6.70	0.84_6	5.85	1.69	5.01	2.54
373.15	14.1	9.8_8	0.98_5	11.0	7.4_0	0.35_8	—	—	—	—	—	—	—
393.15	15.3	10.5_5	0.89_4	12.0	7.8_4	0.32_8	9.6_7	7.5_1	0.66_1	7.2_5	0.91_4	6.14	2.03

The relation between T and r is not known, but will for simplicity, and for purposes of evaluating the effect of the radial gradients upon p_0 and p_l, be taken to be linear. Then

$$\left.\begin{aligned} T_l(r) &= T_l(1-r/a)+T_2(r/a), \\ T_0(r) &= T_0(1-r/a)+T_1(r/a), \end{aligned}\right\} \tag{III. 30}$$

where T_l and T_0 are the temperatures at $x = l$, $r = 0$ and $x = 0$, $r = 0$ respectively and T_2 and T_1 are the temperatures at $x = l$, $r = a$ and $x = 0$, $r = a$. With these relations the steady-state condition ($J = 0$) reduces to

$$\frac{p_0}{p_l} = \frac{\int_0^a (T_l+\Delta(r/a))^{-\frac{1}{2}} r\,\mathrm{d}r}{\int_0^a (T_0-\Delta(r/a))^{-\frac{1}{2}} r\,\mathrm{d}r}, \tag{III. 31}$$

where $\Delta = (T_0-T_1) = (T_2-T_l)$. After integration the final result is

$$\frac{p_0}{p_l} = \frac{T_0^{\frac{1}{2}}}{T_l^{\frac{1}{2}}}\left\{\left(\frac{T_l^2}{T_0^2}\right)\frac{(1+\Delta/T_l)^{\frac{3}{2}}+2-3(1+\Delta/T_l)^{\frac{1}{2}}}{(1-\Delta/T_0)^{\frac{3}{2}}+2-3(1-\Delta/T_0)^{\frac{1}{2}}}\right\}. \tag{III. 32}$$

In our experiments the maximum value of Δ was ~ 5 K when $T_l = 308$ K and $T_0 = 393$ K. With these numbers the correction term in the brace bracket of equation (III. 32) is 0.9904. $(T_0/T_l)^{\frac{1}{2}}$ is the value of p_0/p_l in absence of the radial temperature gradient ($\Delta = 0$). One may conclude that radial gradients of the magnitude arising in the present work have a minimal influence upon p_0/p_l for a non-sorbed Knudsen gas, and in particular cannot account for the values of β for helium given in table III. 1.

Even in thermal transpiration in single capillaries reports of departures from the behaviour of the ideal Knudsen gas have not been uncommon (see, for example, Podgurski & Davis 1961; Edmonds & Hobson 1965). For single capillaries it was reported that roughening the surface or replacing capillaries by apertures served to give pressure ratios equal to the theoretical values for free molecular flow (Edmonds & Hobson 1965; Hobson 1969). Accordingly, since microporous media with tortuous and irregular channel systems represent a more extreme version of roughened capillaries, one would not expect an explanation based on temperature-dependent specular reflexion (Miller & Buice 1966) to be applicable to our results. Wu (1968) discussed the influence of non-Maxwellian distributions of molecular velocities during thermal diffusion of a Knudsen gas and concluded (for temperature gradients in the x-direction only) that $p/\sqrt{T}$ within the capillary would not be constant. An effect of this kind could apply for helium in micropore systems, though according to table 1 of Wu's paper this does not appear to upset the relation $p_l/p_0 = (T_l/T_0)^{\frac{1}{2}}$ in the vessels joined by the capillary. Sandler (1972) suggested that the $\sqrt{T}$ dependence of the isothermal permeability rests upon the assumption that in gas-wall collisions the trajectories of molecules approaching the wall are unchanged by the attraction of the wall. Thus this attraction is assumed to have zero range of action. When more realistic molecule-wall interactions such as the Lennard-Jones 12 : 6 potential are considered the $\sqrt{T}$ dependence may be modified. However, the isothermal helium permeabilities recorded in part II did not deviate signficantly from $\sqrt{T}$ dependence, although the extent of such deviation required for $\beta = 0.72$ is not large and must be considered in relation to experimental uncertainty in measuring both K and β. One may conclude that of several suggestions for explaining values of $\beta \neq 1$ for free molecular flow none can yet be unequivocally regarded as applicable to our results.

III. 4.2. *Interpretation of heats of transport Q_0 and Q_s*

One may first consider Q_s for pure surface flow, J'_s, on an energetically uniform surface. Q_s is next modified to allow for an energetically heterogeneous surface; the argument is extended to the extra flow J_s which is only partially on the surface; and finally Q_0 is obtained for the total flow $J = J_s + J_g$.

Transport occurs from vessel I, in which the gas is maintained at temperature T and pressure p and has molar enthalpy $\tilde{H}_g$, through the microporous membrane to vessel II in which T, p and $\tilde{H}_g$ are infinitesimally different from their values in vessel I. A mol is adsorbed onto the membrane surfaces, on which its molar enthalpy is $\tilde{H}_s$. The adsorbed molecules are then activated so that their enthalpy is increased by the mean amount $\tilde{H}_m$ and they are able to migrate. $\tilde{H}_m$ will be close to the enthalpy of activation ΔH^*. The migrating molecules thus carry enthalpy $\tilde{H}_m + \tilde{H}_s$. The heat of transport, Q_s, is then defined as the heat *absorbed* in vessel I when a mol of gas is added directly to this vessel and a mol is removed by pure surface flow. Thus for Q_s one has

$$Q_s = (\tilde{H}_m + \tilde{H}_s) - \tilde{H}_g = \tilde{H}_m + \Delta\tilde{H}. \tag{III. 33}$$

Here $\Delta\tilde{H}$ is the integral heat of adsorption. From equations (III. 23) and (III. 21):

$$l^s_{12}/l^s_{11} = Q^*_s = Q_s + H^\ominus = \tilde{H}_m + \Delta\tilde{H} + H^\ominus_g. \tag{III. 34}$$

Since $\Delta\tilde{H}$ is negative and $\tilde{H}_m$ is positive but smaller than $-\Delta\tilde{H}$, Q_s must be negative. On the other hand, Q_s is numerically less than $H^\ominus_g$ which is positive, so that Q^*_s is positive.

Equations (III. 33) and (III. 34) give Q_s and Q^*_s for pure surface flow on a uniform surface. If the membrane surface is heterogeneous the effect of heterogeneity may be considered by regarding the surface as composed of a number of patches each energetically uniform, but different from other patches. If $\tilde{H}_i + \Delta\tilde{H}_i$ is the mean enthalpy carried by migrating molecules on the ith kind of patch on which there is a total of n_i adsorbed molecules then Q_s is given by

$$Q_s = \frac{\sum_i n_i(\tilde{H}_i + \Delta\tilde{H}_i)\exp(-E_i/RT)}{\sum_i n_i \exp(-E_i/RT)}, \tag{III. 35}$$

where E_i is the least energy of activation for migration. In this expression $n_i \exp(-E_i/RT) = n'_i$ the number of mobile molecules on the ith kind of patch. Equation (III. 35) assumes that transport on the ith patch is not modified by the juxtaposition of other kinds of patch and so is a first approximation only.

Equation (III. 35) can be re-written as

$$Q_s = \sum_i X'_i(\tilde{H}_i + \Delta\tilde{H}_i), \tag{III. 36}$$

where $X'_i = n'_i/\sum_i n'_i$ and $\sum_i X'_i = 1$. If one writes

$$\sum_i X'_i\tilde{H}_i = \tilde{H}_{av} \quad \text{and} \quad \sum_i X'_i\Delta\tilde{H}_i = \Delta\tilde{H}_{av}$$

then

$$Q_s = \tilde{H}_{av} + \Delta\tilde{H}_{av}. \tag{III. 37}$$

However $\Delta\tilde{H}_{av}$ is not the integral heat of sorption which is $\sum_i X_i\Delta\tilde{H}_i$ where $X_i = n_i/\sum_i n_i$. Also $\tilde{H}_{av}$ is not equal to E_{ss} evaluated in part II in part because E_{ss} refers to all the extra flow J_s and not just to that part of J_s which is in the surface (J'_s), whereas equation (III. 37) refers only to J'_s.

Of J_s we therefore consider that a part $(J_s - J_s') = XJ_s$ is in the gas phase and the part $J_s' = (1-X)J_s$ is on the surface. X is a coefficient such that $0 < X < 1$ (Barrer & Gabor 1960). For the fraction $(1-X)J_s$, Q_s is given by equation (III. 37); while for the fraction XJ_s, the heat of transport is taken to be Q_g. Thus for the extra flow

$$Q_s = (1-X)(\tilde{H}_{av} + \Delta\tilde{H}_{av}) + XQ_g. \tag{III. 38}$$

Finally, for the total flow $J = J_s + J_g$ the overall heat of transport Q_0 when $T = T_0$ is from equation (III. 22)

$$Q_0 = [(1-X)(\tilde{H}_{av} + \Delta\tilde{H}_{av}) + XQ_g]\frac{K_s}{K} + Q_g\frac{K_g}{K}. \tag{III. 39}$$

There is no direct way of evaluating X although estimates have been given for several flow systems which suggest values of *ca.* 0.8 (Barrer & Gabor 1960).

It was shown in part I that Graphon comes nearest to being energetically uniform, in which case equation (III. 39) becomes

$$Q_0 = [(1-X)(\tilde{H}_m + \Delta\tilde{H}) + XQ_g]\frac{K_s}{K} + Q_g\frac{K_g}{K}. \tag{III. 40}$$

It was then assumed that $\tilde{H}_m = -\frac{1}{3}\Delta\tilde{H}$ by analogy with the approximate relation between activation energies for viscous flow in liquids and their latent heat of evaporation (Glasstone *et al.* 1941). For Q_g assumed to be zero the following values of X were found at $T_0/\mathrm{K} = 333.15$ in the Henry law region when $\Delta\tilde{H} = \Delta\tilde{H}^{\ominus}$:

Ar $X = 0.91$,

Kr $X = 0.87$,

Xe $X = 0.73$.

X apparently decreases the more strongly the gas is sorbed, but in view of the assumptions involved further calculations were not made. The values of X are, however, comparable with those estimated by Barrer & Gabor (1960) for isothermal flow of simple paraffins in alumina-silica cracking catalyst membranes.

Again assuming $Q_g = 0$ and also $Q_g = -\frac{1}{2}RT_0$, Q_s and Q_s^* were evaluated from equations (III. 22) and (III. 24) (tables III. 2 and III. 3). The positive values of Q_s^* show the following regularities: all increase with temperature; for a given gas they are larger in Graphon than in Carbolac and for $Q_g = -\frac{1}{2}RT_0$ than for $Q_g = 0$; for the rare gases they decrease in the sequence Ar > Kr > Xe; and, in a given membrane, are larger for polyatomic gases than for monatomic gases. $(\tilde{H}_{av} + \Delta\tilde{H}_{av})$ should be increasingly negative and $(1-X)$ (as seen above) appears to increase in the sequence Ar < Kr < Xe, whereas $H_g^{\ominus}$ at T_0 is the same for all three rare gases. Thus the sequence in Q_s^* is readily understood. $H_g^{\ominus}$ for N_2 and CH_4 exceeds its value for the rare gases so that for comparable values of $(1-X)$ the increase in Q_s^* for these two gases as compared with the rare gases is also consistent.

III. 4.3. *Phenomenological coefficients*

The third of equations (III. 11) serves to evaluate l_{11}^q for helium from the permeability K_g. For helium in all three of the membranes table III. 1 shows that $Q_g^* = 2.14RT_0$ so that $l_{12}^q = Q_g^* l_{11}^q$ is also obtained for this gas (table III. 4). The expression for D_{gs} for Knudsen flow and the relation

between l^g_{11} and D_{gs} (as shown in the third of the equations (III. 12)) gives for l^g_{11} for such flow

$$l^g_{11} = \frac{8\epsilon}{3A}\kappa_{gs}\sqrt{\frac{2}{\pi MRT}}, \tag{III. 41}$$

where κ_{gs} is the structure factor defined by Barrer & Gabor (1959). Equation (III. 41) shows how l^g_{11} is affected by pore properties ($\epsilon\kappa_{gs}/A$), by molecular weight, M, and by temperature.

The relation between l^g_{12} and D_{gs} ($l^g_{12} = (Q^*_g/RT)\,D_{gs}$) shows that l_{12} has the same dimensions as D_{gs} and differs from it numerically by the simple ratio Q^*_g/RT which would be 2, 3 and $\frac{7}{2}$ for an ideal Knudsen gas of monatomic and diatomic molecules and of CH_4 respectively. The ratio for helium, as already seen, is 2.14.

The coefficients l^s_{11} and λ^s_{11} were derived in the Henry law range for other gases using the second of equations (III. 12) with $\mathrm{d}\ln C_g/\mathrm{d}\ln C_s = 1$. Values of δ needed to find C^s/C_s and so to evaluate λ^s_{11} are given in part I, table I. 3. Tables III. 5 and III. 6 exemplify these coefficients and also give the cross-coefficients $l^s_{12} = Q^*_s l^s_{11}$. Two values of l^s_{12} are tabulated corresponding with the two values of Q^*_s based on $Q_g = -\frac{1}{2}RT_0$ and $Q_g = 0$ respectively.

TABLE III. 4. $l^g_{11}/\mathrm{m^2\,s^{-1}\,J^{-1}\,mol}$ AND $l^g_{12}/\mathrm{m^2\,s^{-1}}$ FOR HELIUM IN THE MEMBRANES

	membrane L		membrane M		membrane N	
T_0/K	$10^{10}\,l^g_{11}$	$10^7\,l^g_{12}$	$10^{10}\,l^g_{11}$	$10^7\,l^g_{12}$	$10^9\,l^g_{11}$	$10^6\,l^g_{12}$
308.15	0.78_5	4.3_0	0.78_7	4.3_2	1.47	8.0_4
320.65	0.77_0	4.3_9	0.77_2	4.4_0	1.45	8.2_5
333.15	0.75_3	4.4_7	0.75_7	4.4_9	1.42	8.4_0
343.15	—	—	—	—	1.39	8.5_0
352.90	0.73_2	4.6_0	0.73_7	4.6_2	—	—
353.15	—	—	—	—	1.38	8.6_5
363.15	—	—	—	—	1.35	8.7_5
373.15	—	—	—	—	1.34	8.9_0
378.00	0.71_0	4.7_8	0.70_8	4.7_6	—	—
393.15	—	—	—	—	1.3_0	9.1_1

If the temperature dependence of D_{ss} is expressed by means of the Arrhenius equation $D_{ss} = D_{0s}\exp(-E_{ss}/RT)$ (part II) then the second of equations (III. 12) shows that the temperature coefficient of l^s_{11} is at constant amount sorbed

$$\frac{\partial \ln l^s_{11}}{\partial T} = \frac{E_{ss}-RT}{RT^2} - \frac{\partial}{\partial T}\left[\ln\frac{\mathrm{d}\ln C_g}{\mathrm{d}\ln C_s}\right]. \tag{III. 42}$$

In the Henry law range $\mathrm{d}\ln C_g/\mathrm{d}\ln C_s = 1$ and so the mean activation energy for l^s_{11} is then $E_{ss}-RT$, where E_{ss} is given in part II, table II. 6*a*. The coefficients l^s_{11} of the molecules comprising J_s have therefore the small temperature coefficients shown in tables III. 5 and III. 6. The temperature coefficient of l^s_{12} is given by

$$\frac{\partial \ln l^s_{12}}{\partial T} = \frac{\partial \ln l^s_{11}}{\partial T} + \frac{\partial \ln Q^*_s}{\partial T}. \tag{III. 43}$$

Because Q^*_s has a considerable positive temperature coefficient (tables III. 2 and III. 3) l^s_{12} increases more rapidly with rising temperature than l^s_{11}. For the systems considered in tables III. 5 and III. 6 one also sees that λ^s_{11} and l^s_{11} are numerically similar, reflecting the experimental observation (part I, tables I. 1 and I. 3) that k_s is for the gases involved considerably larger than δ.

Outside the Henry law range λ^s_{11} and l^s_{11} depend upon the amount sorbed. This is shown for

PHILOSOPHICAL TRANSACTIONS OF THE ROYAL SOCIETY A MATHEMATICAL, PHYSICAL & ENGINEERING SCIENCES

TABLE III. 5. PHENOMENOLOGICAL COEFFICIENTS λ^s_{11}, l^s_{11}, l^s_{12} IN THE HENRY LAW RANGE: CARBOLAC MEMBRANES L AND M

units: λ^s_{11}, l^s_{11}: $m^2\ s^{-1}\ J^{-1}\ mol$; l^s_{12}: $m^2\ s^{-1}$

	Ar (L)				Kr (L)				Kr (M)				CH_4 (M)			
			$Q_g = -\frac{1}{2}RT_0$	$Q_g = 0$			$Q_g = -\frac{1}{2}RT_0$	$Q_g = 0$			$Q_g = -\frac{1}{2}RT_0$	$Q_g = 0$			$Q_g = -\frac{1}{2}RT_0$	$Q_g = 0$
T_0/K	$10^{11}\lambda^s_{11}$	$10^{11}l^s_{11}$	$10^7 l^s_{12}$	$10^7 l^s_{12}$	$10^{11}\lambda^s_{11}$	$10^{11}l^s_{11}$	$10^7 l^s_{12}$	$10^7 l^s_{12}$	$10^{11}\lambda^s_{11}$	$10^{11}l^s_{11}$	$10^7 l^s_{12}$	$10^7 l^s_{12}$	$10^{11}\lambda^s_{11}$	$10^{11}l^s_{11}$	$10^7 l^s_{12}$	$10^7 l^s_{12}$
308.15	0.436	0.477	0.223	0.186	0.135	0.138	0.051_0	0.045_6	0.130	0.133	0.044_2	0.039_0	0.292	0.299	0.204	0.191
320.65	0.463	0.515	0.261	0.216	0.161	0.166	0.069_0	0.061_6	0.153	0.157	0.058_5	0.051_4	0.347	0.358	0.264	0.247
333.15	0.479	0.542	0.295	0.242	0.179	0.185	0.082_5	0.073_0	0.167	0.173	0.072_2	0.063_2	0.371	0.386	0.307	0.285
352.90	0.518	0.605	0.364	0.293	0.207	0.217	0.105	0.091_9	0.190	0.200	0.095_8	0.082_9	0.411	0.433	0.386	0.356
378.00	0.573	0.701	0.475	0.378	0.240	0.257	0.139	0.118	0.225	0.242	0.133	0.113	0.469	0.506	0.518	0.472

TABLE III. 6. PHENOMENOLOGICAL COEFFICIENTS λ^s_{11}, l^s_{11}, l^s_{12} IN THE HENRY LAW RANGE: GRAPHON MEMBRANE N

units: λ^s_{11}, l^s_{11}: $m^2\ s^{-1}\ J^{-1}\ mol$; l^s_{12}: $m^2\ s^{-1}$

	N_2				Ar				Kr				Xe			
			$Q_g = -\frac{1}{2}RT_0$	$Q_g = 0$			$Q_g = -\frac{1}{2}RT_0$	$Q_g = 0$			$Q_g = -\frac{1}{2}RT_0$	$Q_g = 0$			$Q_g = -\frac{1}{2}RT_0$	$Q_g = 0$
T_0/K	$10^9\lambda^s_{11}$	$10^9 l^s_{11}$	$10^5 l^s_{12}$	$10^5 l^s_{12}$	$10^9\lambda^s_{11}$	$10^9 l^s_{11}$	$10^5 l^s_{12}$	$10^5 l^s_{12}$	$10^9\lambda^s_{11}$	$10^9 l^s_{11}$	$10^5 l^s_{12}$	$10^5 l^s_{12}$	$10^9\lambda^s_{11}$	$10^9 l^s_{11}$	$10^6 l^s_{12}$	$10^6 l^s_{12}$
308.15	0.374	0.421	0.438	0.334	0.409	0.463	0.369	0.273	0.231	0.242	0.143	0.119	0.096_4	0.0976	0.322	0.279
320.65	0.386	0.441	0.487	0.365	0.413	0.474	0.402	0.291	0.242	0.256	0.167	0.138	0.105	0.106	0.404	0.349
333.15	0.392	0.455	0.531	0.391	0.416	0.485	0.436	0.309	0.248	0.265	0.189	0.155	0.111	0.113	0.498	0.429
343.15	0.393	0.463	0.569	0.413	0.422	0.498	0.468	0.329	0.254	0.273	0.204	0.165	0.116	0.119	0.579	0.498
353.15	0.396	0.472	0.608	0.434	0.417	0.498	0.496	0.344	0.257	0.279	0.222	0.178	0.124	0.127	0.679	0.583
363.15	0.401	0.485	0.654	0.462	0.418	0.506	0.532	0.364	0.262	0.286	0.241	0.192	0.129	0.133	0.776	0.664
373.15	0.403	0.495	0.700	0.489	0.417	0.511	0.560	0.378	0.268	0.295	—	—	0.134	0.138	—	—
393.15	0.411	0.520	0.796	0.548	0.409	0.514	0.617	0.403	0.275	0.308	0.298	0.232	0.145	0.151	1.09_7	0.929

l^s_{11} in figure III. 6 in the cases of CO_2 and C_2H_6 in membrane M and of Xe in membrane L. The curves in this figure approximate to straight lines and show the same kind of steady increase with C'_s as do the diffusion coefficients D_{ss} (part II).

III. 4.4. *Isobaric permeabilities*

The thermo-osmotic steady-state pressure ratio when $J = 0$ is achieved when the flow induced by the temperature difference is just balanced by the reverse flow due to the pressure difference. Since isothermal permeabilities K have been determined at each of a series of temperatures (part II) the thermo-osmotic steady-state should serve to evaluate isobaric permeabilities for which the pressures at $x = 0$ and $x = l$ are made equal but not the temperatures T_0 and T_l. It is of considerable interest to compare the selectivity of permeation for a series of adsorbable molecules under isobaric and isothermal conditions.

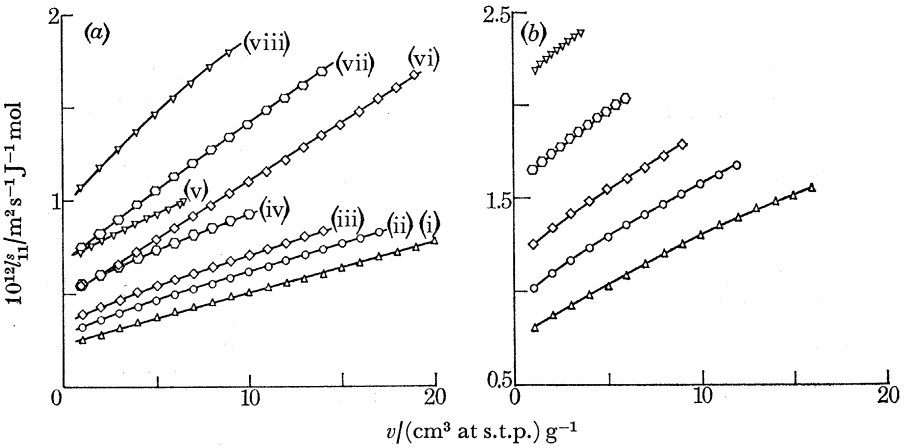

FIGURE III. 6. l^s_{11} as a function of amount sorbed. △, 308.15 K; ○, 320.65 K; ◇, 333.15 K; ⬡, 352.90 K; ▽, 378.00 K. (*a*) Curves (i) to (v), Xe in L; curves (vi) to (viii), C_2H_6 in M. (*b*) CO_2 in M.

So long as K is independent of C_g the flux in mol s^{-1} per unit cross-section may be rewritten as

$$J = -\frac{K}{RT}\left[p\frac{Q}{RT^2} + \frac{\mathrm{d}p}{\mathrm{d}T}\right]\frac{\mathrm{d}T}{\mathrm{d}x}. \tag{III. 44}$$

By multiplying K by $\exp\left[-\int_{T_l}^{T}\frac{Q}{RT^2}\mathrm{d}T\right]$

and each term in the square bracket by

$$\exp\left[\int_{T_l}^{T}\frac{Q}{RT^2}\mathrm{d}T\right]$$

this equation becomes

$$J = -\left\{\frac{K}{RT}\exp\left[-\int_{T_l}^{T}\frac{Q}{RT^2}\mathrm{d}T\right]\right\}\frac{\mathrm{d}}{\mathrm{d}x}\left[p\exp\left[\int_{T_l}^{T}\frac{Q}{RT^2}\mathrm{d}T\right]\right]. \tag{III. 45}$$

In this relation T may be varied but T_l must be fixed. For a steady state in which J is constant the term in the brace bracket may be brought to the left-hand side of the equation and both sides integrated, first from 0 to l and then from x to l. The following two expressions for J then result:

$$J = \frac{p_0\exp\left[\int_{T_l}^{T_0}\frac{Q}{RT^2}\mathrm{d}T\right] - p_l}{\int_0^l\left\{\frac{RT}{K}\exp\left[\int_{T_l}^{T}\frac{Q}{RT^2}\mathrm{d}T\right]\right\}\mathrm{d}x} = \frac{p(x)\exp\left[\int_{T_l}^{T}\frac{Q}{RT^2}\mathrm{d}T\right] - p_l}{\int_x^l\left\{\frac{RT}{K}\exp\left[\int_{T_l}^{T}\frac{Q}{RT^2}\mathrm{d}T\right]\right\}\mathrm{d}x}. \tag{III. 46}$$

The energy flow at T_0, $G(T_0)$ is related to J, at this temperature, in both cases per unit cross-section, by

$$G(T_0) = RT_0 J.$$

One may then define a coefficient $B(T_0)$ by

$$B(T_0) = \frac{RT_0 Jl}{\Delta T} = \frac{RT_0 l}{\Delta T} \frac{p_0 \exp\left[\int_{T_l}^{T_0} \frac{Q}{RT^2} \mathrm{d}T\right] - p_l}{\int_0^l \left\{\frac{RT}{K} \exp\left[\int_{T_l}^{T} \frac{Q}{RT^2} \mathrm{d}T\right] \mathrm{d}x\right\}}, \tag{III. 47}$$

where $\Delta T = (T_0 - T_l)$. Since $\mathrm{d}T/\mathrm{d}x = -(T_0 - T_l)/l$ this relation reduces to

$$\frac{B(T_0)}{p_0} = \frac{T_0 \left\{\exp\left[\int_{T_l}^{T_0} \frac{Q}{RT^2} \mathrm{d}T\right] - \frac{p_l}{p_0}\right\}}{\int_{T_l}^{T_0} \left\{\frac{T}{K} \exp\left[\frac{Q}{RT^2} \mathrm{d}T\right]\right\} \mathrm{d}T}. \tag{III. 48}$$

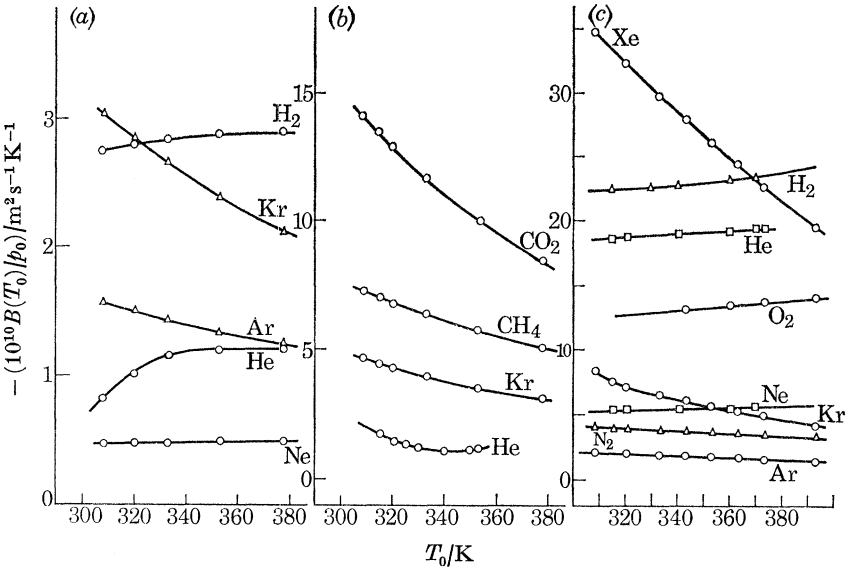

FIGURE III. 7. $-B(T_0)/p_0$ as a function of T_0. (*a*) Membrane L; (*b*) membrane M; (*c*) membrane N.

For the isobaric condition $p_l = p_0$. Also from equation (III. 18)

$$\exp\left[\int_{T_l}^{T_0} \frac{Q}{RT^2} \mathrm{d}T\right] = \left(\frac{p_l}{p_0}\right)_{J=0} \quad \text{and} \quad \exp\left[\int_{T_l}^{T} \frac{Q}{RT^2} \mathrm{d}T\right] = \left(\frac{p_l}{p(x)}\right)_{J=0},$$

so that the isobaric permeability is

$$-\frac{B(T_0)}{p_0} = \frac{T_0[1 - (p_l/p_0)_{J=0}]}{\int_{T_l}^{T_0} \left\{\frac{T}{K}\left(\frac{p_l}{p(x)}\right)_{J=0}\right\} \mathrm{d}T}. \tag{III. 49}$$

The integral may be evaluated by plotting T/K and the pressure ratios p_0/p_l for $J = 0$ against T. At a temperature T one may read off $(p_l/p(x))_{J=0}$ and T/K. The product of these quantities is in turn plotted against T and the area under this curve between the limits T_l and T_0 is the integral in the denominator of the expression for $B(T_0)/p_0$.

The isobaric permeabilities are shown as functions of T_0 in figure III. 7. For the more strongly adsorbed gases $-B(T_0)/p_0$ decreases as T_0 increases, the slopes increasing with sorbability. For various pairs of gases the ratios of isobaric permeabilities may have very different magnitudes from the ratios of isothermal permeabilities, as shown by the values in table III. 7. For the Graphon membrane the isobaric ratios are particularly favourable for separations as compared with isothermal ratios, although in each case for actual separations cross-coefficients between the flows of each component of a mixture must be taken into account.

TABLE III. 7. RATIOS OF ISOBARIC AND OF ISOTHERMAL PERMEABILITIES FOR PAIRS OF GASES

gas pair (A/B)	temperature T_0/K	isobaric ratio (A/B)	isothermal ratio (A/B)
	(*a*) membrane L		
Ar/Ne	320.65	3.14	1.49
	378.00	2.54	1.29
Kr/Ne	320.65	5.97	1.61
	378.00	4.34	1.25
H_2/Ne	320.65	5.82	3.60
	378.00	5.93	3.50
Kr/Ar	320.65	1.90	1.08
	378.00	1.71	0.97
	(*b*) membrane M		
CH_4/Kr	320.65	1.60	2.14
	378.00	1.66	2.12
CO_2/Kr	320.65	3.02	2.39
	378.00	2.75	2.03
CO_2/CH_4	320.65	1.89	1.12
	378.00	1.66	0.96
H_2/Ar	320.65	1.86	2.42
	378.00	2.33	2.71
H_2/Kr	320.65	1.03	2.23
	378.00	1.37	2.80
	(*c*) membrane N		
N_2/Ar	320.65	1.93	1.13
	393.15	2.27	1.14
Kr/Ar	320.65	3.54	0.96
	393.15	3.03	0.87
Xe/Ar	320.65	16.2	1.25
	393.15	14.2	0.97
Kr/N_2	320.65	1.84	0.85
	393.15	1.34	0.76
Xe/N_2	320.65	8.41	1.11
	393.15	6.26	0.85
Xe/Kr	320.65	4.58	1.30
	393.15	4.68	1.12

III. 4.5. *Pressure distributions within the membranes*

For any constant value of J, equation (III. 46) gives the pressure distribution, $p(x)$, across the membrane. This equation in conjunction with equation (III. 18) gives

$$\frac{\dfrac{p_0}{p_l}\left(\dfrac{p_l}{p_0}\right)_{J=0}-1}{\displaystyle\int_0^l\left\{\frac{T}{K}\left(\frac{p_l}{p(x)}\right)_{J=0}\right\}\mathrm{d}x}=\frac{\left(\dfrac{p(x)}{p_l}\right)\left(\dfrac{p_l}{p_0}\right)_{J=0}-1}{\displaystyle\int_x^l\left\{\frac{T}{K}\left(\frac{p_l}{p(x)}\right)_{J=0}\right\}\mathrm{d}x}$$

which for a linear temperature gradient reduces to

$$\frac{\left(\frac{p_0}{p_l}\right)\left(\frac{p_l}{p_0}\right)_{J=0}-1}{\int_{T_l}^{T_0}\left\{\frac{T}{K}\left(\frac{p_l}{p(x)}\right)_{J=0}\right\}\mathrm{d}T}=\frac{\left(\frac{p(x)}{p_l}\right)\left(\frac{p_l}{p(x)}\right)_{J=0}-1}{\int_{T_l}^{T}\left\{\frac{T}{K}\left(\frac{p_l}{p(x)}\right)_{J=0}\right\}\mathrm{d}T}. \tag{III. 50}$$

The integrals in this equation can be evaluated following the procedure given in the preceding section (III. 4.4). For isobaric transport ($p_0 = p_l$) some values of $p(x)/p_l$ were calculated and are shown as functions of x/l in figure III. 8. For all the gases so examined the ratio $p(x)/p_l$ is greater than unity for $0 < x < l$. The curves are almost parabolic in form with maxima in $p(x)/p_l$ which increase with sorbability of the gas.

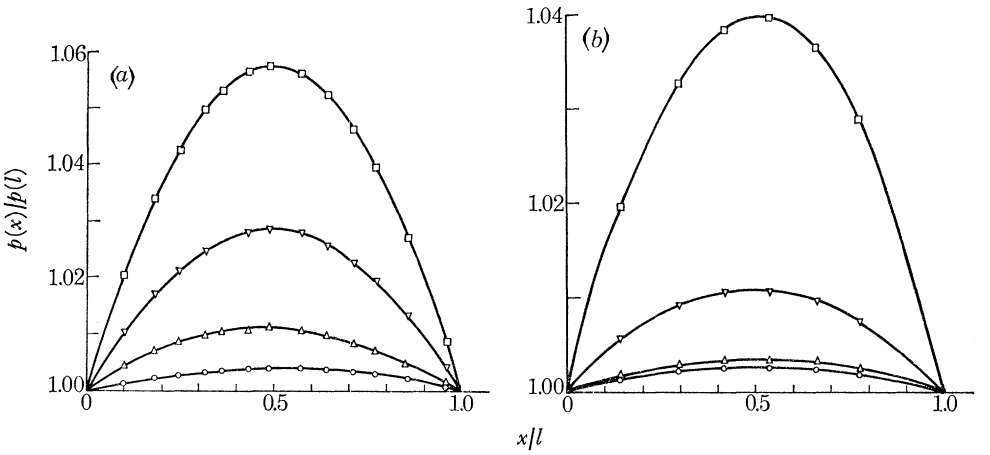

FIGURE III. 8. Pressure profiles for steady-state isobaric transport. (*a*) $T_l = 308.15\,\mathrm{K}$, $T_0 = 378.0\,\mathrm{K}$. □, CO_2 in M; ▽, CH_4 in M; △, Ar in L; ○, H_2 in L. (*b*) Membrane N: $T_l = 308.15\,\mathrm{K}$, $T_0 = 393.15\,\mathrm{K}$; □, Xe; ▽, Kr; △, N_2; ○, Ar.

If, as experimentally observed, with several weakly sorbed gases (III. 4.1), the heat of transport is given by the simple relation $Q = -\frac{1}{2}\beta RT$, then the integrations in the experimental terms of equation (III. 46) may readily be made and lead to

$$J=\frac{p_0/T_0^{\frac{1}{2}\beta}-p_l/T_l^{\frac{1}{2}\beta}}{\int_0^l\frac{RT^{(1-\frac{1}{2}\beta)}}{K}\mathrm{d}x}=\frac{p(x)/T^{\frac{1}{2}\beta}-p_l/T_l^{\frac{1}{2}\beta}}{\int_0^l\frac{RT^{(1-\frac{1}{2}\beta)}}{K}\mathrm{d}x}. \tag{III. 51}$$

When $\beta = 1$ (an ideal Knudsen gas) K is proportional to $\sqrt{T}$ and so this expression becomes

$$\frac{p_0/T_0^{\frac{1}{2}}-p_l/T_l^{\frac{1}{2}}}{l}=\frac{p(x)/T^{\frac{1}{2}}-p_l/T_l^{\frac{1}{2}}}{l-x}. \tag{III. 52}$$

This accords with kinetic theory as developed, for example, by Kennard (1938).

III. 4.6. *Thermo-osmotic counter flows on surfaces and in the gas phase*

In the thermo-osmotic steady state with $J = 0 = J'_s + J'_g = J_s + J_g$, two possibilities arise for the components J'_s, J'_g or J_s, J_g:

Case 1. The condition $J = 0$ is satisfied when

$$J'_s = 0,\ J'_g = 0, \quad J_s = 0,\ J_g = 0.$$

For an ideal Knudsen gas the steady-state condition for J'_g (or J_g) corresponds with

$$p_0/p_l = \sqrt{(T_0/T_l)}.$$

This condition must separately satisfy $J'_s = 0$ (or $J_s = 0$), and one must then have (Ash & Barrer 1963)

$$\frac{l^s_{12}}{l^s_{11}} = \frac{l^g_{12}}{l^g_{11}}, \quad \text{i.e. } Q^*_s = Q^*_g.$$

However, for adsorbed gases the properties of the thermo-osmotic steady state $J = 0$ are quite different from those of a Knudsen gas (figure III. 5), and case 1 cannot give a general explanation of our results.

Case 2. Alternatively when $J = 0$ we may have

$$J'_s = -J'_g \quad \text{or} \quad J_s = -J_g.$$

In this case there are equal and opposite counterflows on the surface and in the gas phase through each cross-section. This condition requires that $J'_s/J'_g = -1$, but J'_s and J'_g can vary with x provided only that they remain equal and opposite. For case 2 a satisfactory explanation of the behaviour of p_0/p_l when $J = 0$ (figure III. 4) is possible in terms of equations (III. 18) and (III. 22). It thus seems that equal and opposite counterflows in surface and gas phase will in general characterize the thermo-osmosis of sorbable gases.

Such counterflows with exchange of molecules between flows can be of interest for mixture separation where J'_s occurs in a dense film (Lassettre & Brooks 1961). The counterflows recall in certain respects the conditions in distillation columns with total reflux.

III. 5. *Conclusion*

It has been possible to treat both experimentally and theoretically most aspects of thermo-osmosis of sorbable gases and vapours in microporous membranes. Adequate interpretation is possible only when parallel studies of adsorption equilibria and of isothermal transport have also been made, because of the inter-connexion of the three aspects of membrane physics. Accordingly, the work reported here is considerably more complete then any previous study.

We are indebted to Dr T. Foley for the numerical calculations of §§ III. 4.4 and 4.5.

Acknowledgement is made to the Science Research Council for awards to J. H. C., R. J. D. and C. L. M. which made possible their participation in this programme.

References

Ash, R., Baker, R. W. & Barrer, R. M. 1967 *Proc. R. Soc. Lond.* A **299**, 434.
Ash, R., Baker, R. W. & Barrer, R. M. 1968 *Proc. R. Soc. Lond.* A **304**, 407.
Ash, R. & Barrer, R. M. 1963 *Trans. Faraday Soc.* **59**, 2260.
Ash, R., Barrer, R. M. & Lowson, R. T. 1970 *Surface Sci.* **21**, 265.
Ash, R., Barrer, R. M. & Pope, C. G. 1963*a* *Proc. R. Soc. Lond.* A **271**, 1.
Ash, R., Barrer, R. M. & Pope, C. G. 1963*b* *Proc. R. Soc. Lond.* A **271**, 19.
Aylmore, L. A. G. & Barrer, R. M. 1966 *Proc. R. Soc. Lond.* A **290**, 477.
Barrer, R. M. 1963 *Can. J. Chem.* **41**, 1768.
Barrer, R. M. 1967 *The solid-gas interface* (ed. E. A. Flood), vol. 2, ch. 19. New York: Marcel Dekker Inc.
Barrer, R. M. 1970 *Proc. Int. Symp. on Surface Area Determination* (*Bristol* 1969), p. 277. London: Butterworths.
Barrer, R. M. & Gabor, T. 1959 *Proc. R. Soc. Lond.* A **251**, 353.

PHILOSOPHICAL TRANSACTIONS OF THE ROYAL SOCIETY A MATHEMATICAL, PHYSICAL & ENGINEERING SCIENCES

Barrer, R. M. & Gabor, T. 1960 *Proc. R. Soc. Lond.* A **256**, 267.
Barrer, R. M. & Papadopoulos, R. 1972 *Proc. R. Soc. Lond.* A **326**, 315.
Barrer, R. M. & Rees, L. V. C. 1959 *Trans. Faraday Soc.* **55**, 992.
Barrer, R. M. & Rees, L. V. C. 1961 *Trans. Faraday Soc.* **57**, 999.
Barrer, R. M. & Strachan, E. 1955 *Proc. R. Soc. Lond.* A **231**, 52.
Carman, P. C. & Malherbe, P. le R. 1950 *Proc. R. Soc. Lond.* A **203**, 165.
Carman, P. C. & Raal, F. A. 1951 *Proc. R. Soc. Lond.* A **209**, 59.
Crowe, C. M. 1957 *Trans. Faraday Soc.* **53**, 1413.
de Boer, J. H. & Custers, J. F. H. 1934 *Z. Phys. Chem.* **25**, 225.
Denbigh, K. G. 1951 *The thermodynamics of the steady state*. London: Methuen.
Edmonds, T. & Hobson, J. P. 1965 *J. Vac. Sci. Tech.* **2**, 182.
Everett, D. H. 1950 *Trans. Faraday Soc.* **46**, 957.
Frank, H. S. 1945 *J. Chem. Phys.* **13**, 493.
Gilliland, E. R., Baddour, R. F. & Engal, H. H. 1962 *A.I.Ch.E. J.* **8**, 530.
Gilliland, E. R., Baddour, R. F. & Russell, J. L. 1958 *A.I.Ch.E. J.* **4**, 90.
Glasstone, S., Laidler, K. J. & Eyring, H. 1941 *The theory of rate processes*, p. 198. New York: McGraw-Hill.
Guggenheim, E. A. 1926 *Phil. Mag.* (7) **2**, 538.
Hanley, H. J. M. 1965 *J. Chem. Phys.* **43** 1510.
Hanley, H. J. M. 1966 *Trans. Faraday Soc.* **62**, 2395.
Hill, T. L. 1952 *Advances in catalysis*, p. 211. New York: Academic Press Inc.
Hill, T. L. 1956 *J. Chem. Phys.* **25**, 730.
Hobson, J. P. 1969 *J. Vac. Sci. Tech.* **6**, 257.
Hopfinger, E. J. & Altman, M. 1969 *J. Chem. Phys.* **50**, 2417.
Kammermeyer, K. & Rutz, L. O. 1959 *Chem. Eng. Progr. Symp. Ser.* no. 24 **55**, 163.
Kennard, E. H. 1938 *Kinetic theory of gases*, p. 330. New York: McGraw-Hill.
Kirkwood, J. G. 1932 *Phys. Z.* **33**, 57.
Lassettre, E. N. & Brooks, A. A. 1961 Unclassified Report K-1464.
London, F. 1930 *Z. Phys.* **63**, 245.
Miller, G. A. & Buice, R. L. 1966 *J. Phys. Chem.* **70**, 3874.
Müller, A. 1936 *Proc. R. Soc. Lond.* A **154**, 624.
Podgurski, H. H. & Davis, F. N. 1961 *J. Phys. Chem.* **65**, 1343.
Rastogi, R. P., Singh, K. & Singh, H. P. 1969 *J. Phys. Chem.* **73**, 2798.
Rossman, R. P. & Smith, W. R. 1943 *Ind. Eng. Chem.* **35**, 972.
Sandler, S. I. 1972 *Ind. Eng. Chem. Fundam.* **11**, 424.
Saylor, J. H. & Battino, R. 1958 *J. Phys. Chem.* **62**, 1334.
Slater, J. C. & Kirkwood, J. G. 1931 *Phys. Rev.* **37**, 682.
Wright, P. G. 1971 *Trans. Faraday Soc.* **67**, 2551.
Wu, Y. 1968 *J. Chem. Phys.* **48**, 889.
Young, D. M. & Crowell, A. D. 1962 *Physical adsorption of gases*, ch. 2. London: Butterworths.

PHILOSOPHICAL TRANSACTIONS OF THE ROYAL SOCIETY A MATHEMATICAL, PHYSICAL & ENGINEERING SCIENCES